CHAPTER III

RESULTS AND DISCUSSION

At present, the research towards the discovery and development of new agrochemicals are still called for, particularly for management. The search for natural-product-based agrochemicals has intensified recently, as they are biodegradable, eco-friendly, and safe to the environment. Moreover in view of the ecotoxicity of synthetic insecticides and resistance developed by the insects, antifeedants offer considerable promise as components of emerging integrated pest management (IPM) due to their capacity to reduce feeding by insect.[6] In addition, Thailand is an agricultural country and a part of the Southeast Asia where abounds in plant species. It should be a potent source for active principle for this regards. Therefore, the preliminary screening for agrochemicals from seventeen Thai plants was conducted.

3.1 The results of preliminary screening extraction

Seventeen Thai plants were extracted with dichloromethane and methanol by the general procedure described in Chapter II. The results of extraction are presented in Table 3.1.

Table 3.1 The results of extraction of selected seventeen Thai plants

Name	Part	Weight of dried plants (g)	Crude extract (g) (% wt by wt)	
			CH_2Cl_2	MeOH
Betula alnoides Buch. Ham.	Leaves	550	16.40 (2.98)	30.18 (5.49)
Cyperus alternifolius Roxb.	Leaves	810	3.08 (0.38)	18.23 (2.25)
Cyperus rotundus L.	Tubers	950	20.28 (2.13)	42.19 (4.44)
Artocarpus heterophyllus Lam.	Heartwood	900	13.86 (1.54)	13.18 (1.46)
Cinnamomum subavenium Miq.	Heartwood	880	3.05 (0.35)	10.43 (1.18)
Pterocarpus macrocarpus Kurz.	Heartwood	900	10.82 (1.20)	47.47 (5.27)
Tectona grandis L. F.	Heartwood	950	37.79 (3.98)	17.27 (5.40)
Alpinia galanga (Linn.) Swarts	Rhizome	940	24.71 (2.63)	23.8 (2.53)
Amomum xanthioides Walls	Rhizome	1000	10.04 (1.00)	19.05 (1.90)
Kaempferia galanga L.	Rhizome	850	19.92 (2.34)	6.74 (0.79)
Zingiber cassumunar Roxb.	Rhizome	950	32.86 (3.46)	9.93 (1.04)
Zingiber zerumbet (Linn.) Smith	Rhizome	890	16.16 (1.82)	16.03 (1.80)
Xylia xylocarpa Taub.	Heartwood	900	19.27 (2.14)	36.60 (4.07)
Anamirta cocculus (L.)	Heartwood	1000	2.15 (0.22)	18.89 (1.89)
Anaxagorea luzonensis Gray.	Heartwood	950	10.71 (1.13)	8.65 (0.91)
Cryptolepis buchanani Roem, Schult.	Heartwood	900	9.96 (1.11)	5.27 (0.59)
Ventilago denticulate Willd.	Heartwood	1300	10.43 (0.80)	16.52 (1.27)

According to the above results, the highest amount of methanol and dichloromethane extracts (% weight by weight) was achieved from the leaves of *B. alnoides* and the heartwood of *T. grandis*, respectively.

3.2 The results of biological activity screening test

Both dichloromethane and methanol crude extracts of the aforementioned plants were preliminarily screened for their insect antifeedant activity against *S. litura* and phytotoxicity against lettuce seedlings in accordance with the procedures described in Chapter II. The results are demonstrated in Tables 3.2 and 3.3.

Table 3.2 Insect antifeedant indices of selected seventeen plants

Species	Solvent	AFI	SD	FI (%)	CDC (%)
Anaxagorea luzonensis Gray.	CH_2Cl_2	40.9	12.86	18.2	100.0
	MeOH	ND	ND	ND	ND
Cryptolepis buchanani Roem, Schult.	CH_2Cl_2	41.2	12.49	17.7	100.0
	MeOH	ND	ND	ND	ND
Betula alnoides Buch. Ham.	CH_2Cl_2	inactive	-----	-----	100.0
	MeOH	inactive	-----	-----	100.0
Cyperus alternifolius Roxb.	CH_2Cl_2	36.6	8.51	26.9	100.0
	MeOH	46.1	5.52	7.8	100.0
Cyperus rotundus L.	CH_2Cl_2	inactive	-----	-----	100.0
	MeOH	42.6	10.47	14.8	100.0
Cinnamomum subavenium Miq.	CH_2Cl_2	inactive	-----	-----	100.0
	MeOH	inactive	-----	-----	100.0
Pterocarpus macrocarpus Kurz.	CH_2Cl_2	8.9	9.49	82.2	83.6
	EtOH	inactive	-----	-----	100.0
Xylia xylocarpa Taub.	CH_2Cl_2	3.5	5.00	92.9	16.9
	EtOH	46.9	3.98	6.3	83.3
Anamirta cocculus (L.)	CH_2Cl_2	47.4	3.66	5.2	100.0
	MeOH	15.7	4.25	68.5	46.2
Artocarpus heterophyllus Lam.	CH_2Cl_2	4.8	6.73	90.5	63.0
	MeOH	43.1	1.17	13.9	100.0
Ventilago denticulata Willd.	CH_2Cl_2	23.9	6.73	52.3	100.0
	MeOH	49.8	0.25	0.4	88.2
Tectona grandis L. F.	CH_2Cl_2	27.7	13.93	44.7	74.5
	EtOH	17.6	4.52	64.8	100.0
Alpinia galanga (Linn.) Swarts	CH_2Cl_2	33.7	0.87	32.6	85.6
	MeOH	40.9	5.86	18.2	100.0
Amomum xanthioides Walls	CH_2Cl_2	42.6	2.5	14.8	69.2
	MeOH	42.3	26.7	15.4	49.7
Kaempferia galanga L.	CH_2Cl_2	6.8	9.58	86.5	100.0
	MeOH	16.8	7.22	66.3	100.0
Zingiber cassumunar Roxb.	CH_2Cl_2	7.7	10.88	84.6	20.2
	MeOH	5.7	8.08	88.6	55.6
Zingiber zerumbet (Linn.) Smith	CH_2Cl_2	37.7	1.45	24.6	100.0
	MeOH	inactive	-----	-----	100.0

ND = not determined; Applied dose is 1.0 mg / disk

Table3.3 Effects of selected plants on lettuce seedling

Species	Solvent	phytotoxicity	Symptom
Anaxagorea luzonensis Gray.	CH_2Cl_2	Inactive	
	MeOH	Slightly	
Cryptolepis buchanani Roem, Schult.	CH_2Cl_2	Inactive	
	MeOH	Inactive	
Betula alnoides Buch. Ham.	CH_2Cl_2	Strong	Necrosis
	MeOH	Strong	
Cyperus alternifolius Roxb.	CH_2Cl_2	Inactive	
	MeOH	Inactive	
Cyperus rotundus L.	CH_2Cl_2	Inactive	
	MeOH	Inactive	
Cinnamomum subavenium Miq.	CH_2Cl_2	Slightly	
	MeOH	Slightly	
Pterocarpus macrocarpus Kurz.	CH_2Cl_2	Inactive	Radicle elongation
	MeOH	Slightly	Dying
Xylia xylocarpa Taub.	CH_2Cl_2	Inactive	Radicle elongation
	MeOH	Slightly	Dying
Anamirta cocculus (L.)	CH_2Cl_2	Inactive	
	MeOH	Slightly	
Artocarpus heterophyllus Lam.	CH_2Cl_2	Inactive	Radicle elongation
	MeOH	Slightly	Dying
Ventilago denticulata Willd.	CH_2Cl_2	Slight	Chlorosis
	MeOH	Slightly	Dying
Tectona grandis L. F.	CH_2Cl_2	Inactive	
	MeOH	Inhibition	Chlorosis
Alpinia galanga (Linn.) Swarts	CH_2Cl_2	Strong	Chlorosis
	MeOH	Inhibition	Chlorosis
Amomum xanthioides Walls	CH_2Cl_2	Slightly	
	MeOH	Slightly	
Kaempferia galanga L.	CH_2Cl_2	Strong	Necrosis
	MeOH	Strong	
Zingiber cassumunar Roxb.	CH_2Cl_2	Inactive	
	MeOH	Slightly	Dying
Zingiber zerumbet (Linn.) Smith	CH_2Cl_2	Slight	
	MeOH	Inactive	

Data shown represent the observation of two replicates. Applied dose is 1000 ppm.

As the results of screening tests, most of the dichloromethane extracts displayed more antifeedant activity than the methanol extracts. Among them, the dichloromethane extract of *P. macrocarpus*, *X. xylocarpa*, *A. heterophyllus*, *K. galanga* and both extracts of *Z. cassumunar* showed strong antifeedant activity against the common cutworm, while the methanol extracts from *A. cocculus*, *T. grandis* and *K. galanga* exhibited moderate activity.

The control disk consumption value displayed the feeding deterrent capacity of the antifeedants. The strong antifeedants should express low values of the control disk consumption percentage because they could inhibit feeding of insects not only the treat disk, but also the control disk. As for the results, the dichloromethane extracts of *X. xylocarpa* and *Z. cassumunar* exhibited interesting results of %CDC value at 16.9 and 20.2, respectively.

The effects of all crude extracts on the growth of lettuce seeds were investigated to look for the substances that did not show the side effect on plants. The results showed that both extracts of *C. buchanani*, *C. alternifolius*, *C. rotundus* and the dichloromethane extracts of *A. luzonensis*, *P macrocarpus*, *X. xylocarpa*, *A. cocculus*, *A. heterophyllus*, *T. grandis* and *Z. cassumunar* did not exhibit the inhibitory effect on the growth of lettuce seeds.

As mentioned above, the dichloromethane extract from the heartwood of *X. xylocarpa* exhibited the best antifeedant activity against *S. litura* (%FI = 92.9). In addition, it was observed that the common cutworm did not consume the control disk (%CDC = 16.9). Moreover this extract did not show the phytotoxicity against lettuce seedling. These results supported that this crude extract revealed potent feeding inhibition with no effect on the crops. Therefore, the heartwood of *X. xylocarpa* was chosen for further investigation on the chemical constituents and searching for insect antifeedant compounds.

3.3 The results of the extraction of the heartwood of *X. xylocarpa*

The heartwood of *X. xylocarpa* was extracted by various solvents according to the procedure described in Chapter II. The results of the extraction of the heartwood of *X. xylocarpa* are shown in Table 3.4.

Table 3.4 The results of extraction of the heartwood of *X. xylocarpa* (7 Kg)

Crude extract	Fraction	Weight (g)	% w/w
Hexane	I	166.42	2.38
Dichloromethane	II	75.03	1.07
Ethyl acetate	III	94.54	1.35
Methanol	IV	256.06	3.66

From the extraction results, it was signified that the best yield was gained from the methanol extract 256.06 g or 3.66 % (w/w), the second was the hexane crude extract.

The hexane and dichloromethane crude extracts were preliminarily checked on their chemical constituents by TLC using 10% ethyl acetate in hexane as a solvent system. The results are displayed as shown below.

I II

I = Hexane extract, II = Dichloromethane extract

Solvent system; Hexane:EtOAc 9:1

The TLC results clearly revealed that the hexane extract contained almost the same constituents as those in the less polar part of dichloromethane extract.

3.4 The results of *X. xylocarpa* antifeedant activity test

The hexane, dichloromethane, ethyl acetate and methanol crude extracts of *X. xylocarpa* were preliminarily screened for the antifeedant activity against *S. litura* according to the procedures described in Chapter II. The results are demonstrated in Table 3.5.

Table 3.5 Insect antifeedant indices of hexane, CH_2Cl_2, EtOAc and MeOH crude extract

Crude extract	AFI	FI(%)	SD
Hexane	31.1	37.7	16.7
CH_2Cl_2	15.4	69.9	1.67
EtOAc	29.6	40.9	0.2
MeOH	47.0	5.9	7.4

Applied dose is 1.0 mg / disk

According to the above results, although the dichloromethane extract exhibited the best antifeedant activity, the feeding inhibitory value of this extract decreased from the previous examination (%FI = 92.9), while the hexane and ethyl acetate extracts exhibited moderate antifeedant activity. This suggested that some active compounds in dichloromethane extract be partitioned into hexane and ethyl acetate extracts. The activity was therefore depended on the constituents and the amount of active ingredients present in the extract. Thus, the separation of dichloromethane extract was considered for further study.

3.5 The separation of dichloromethane crude extract

The portion of dichloromethane extract (Fraction II), 40 g as yellow oil was chromatographed on silica gel column chromatography using Merck's silica gel 60 Art 7734 as an adsorbent. The column was initially eluted with hexane and increasing polarity by mixing with ethyl acetate, following by methanol in ethyl acetate. The eluted solution was collected and concentrated by vacuum. Then the portion was checked by TLC, and the fractions that showed similar components were combined. The results of separation are shown in Table 3.6 and Scheme 3.1.

Table 3.6 The separation of dichloromethane crude extract (Fraction II)

Fraction	Eluent (% vol/vol)	Remarks	Weight (g)
IIA	100% Hexane	Colorless oil	0.52
IIB	2% EtOAc-Hexane	White solid (compound **1**)	7.75
IIC	2% EtOAc-Hexane	Yellow pale solid	2.65
IID	8% EtOAc-Hexane	White solid	2.01
IIE	8% EtOAc-Hexane	White solid	7.40
IIF	10% EtOAc-Hexane	Yellow brown oil	2.25
IIG	50% EtOAc-Hexane	Yellow solid (compound **2**)	0.74

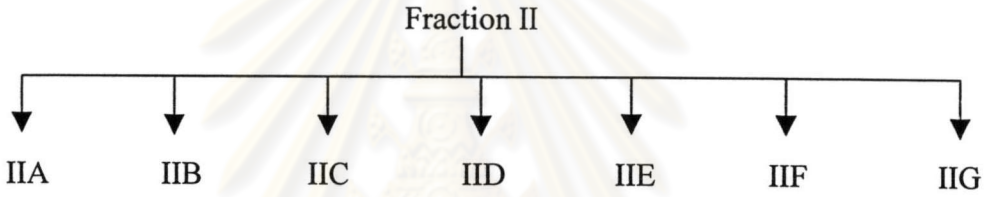

Scheme 3.1 The separation of dichloromethane extract

As the results, the separation of dichloromethane extract yielded 7 fractions **(IIA-IIG)**. After recrystallization of Fraction IIB with methanol, compound **1** as white platelet was obtained. The solid containing in Fraction IIG was purified by first washing with cooled ethyl acetate and then recrystallized with ethyl acetate. The colorless crystal was afforded, designated as compound **2**.

Structural elucidation of compound 1

After recrystallization Fraction IIB with methanol, white platelet compound (6.50 g, 16.50 %yield) designated as compound **1** exhibited a single spot on TLC with R_f value 0.56 (10% ethyl acetate in hexane), m.p. 51-52 °C. This compound immediately gave a blue spot after dipping in 10%H_2SO_4 in ethanol and was soluble in hexane, dichloromethane and ethyl acetate, and slightly soluble in methanol.

The IR spectrum (Figure 1) showed the characteristic absorption peaks of carbonyl group at 1700 cm^{-1} (C=O) and a vinyl group at 3081, 1634, 999 and 914 cm^{-1}. The C=C stretching vibration of alkene displayed an absorption peak at 1634

cm^{-1}. In addition, the C-H asymmetric bending of CH_3 (gem-dimethyl) was observed at 1385 cm^{-1}.

The mass spectrum (Figure 2) exhibited the molecular ion peak at *m/z* 286 [M^+] along with important fragment ion peaks at *m/z* 271, 258 and 135. Molecular formula of this compound was determined to be $C_{20}H_{30}O$ on the basis of ^1H, ^{13}C-NMR and mass spectral data, indicating 6 degrees of unsaturation.

The ^1H-NMR spectrum and signal integration ($CDCl_3$, Figure 3) established the presence of four tertiary methyl groups at δ 1.11 (s, CH_3), 1.08 (s, $2xCH_3$) and 1.02 (s, CH_3), an olefinic proton as a sharp singlet at δ 5.31 and three signals of an ABX system corresponding to three vinyl protons from the mono-substituted double bond at δ 5.78 (1H, dd, J = 17.4 and 10.5 Hz), 4.93 (1H, dd, J = 17.4 and 1.7 Hz) and 4.92 (1H, dd, J = 10.5 and 1.7 Hz). This proton spectrum pattern was well matched with the skeleton of pimarane type diterpenoids that commonly found in the heartwood of *Xylia dolabriformis*.[23] In addition, as the olefinic proton (5.31 ppm) appeared as a sharp singlet, it could only be placed at C14 in association with a C8-C14 double bond in a normal pimarane type skeleton.

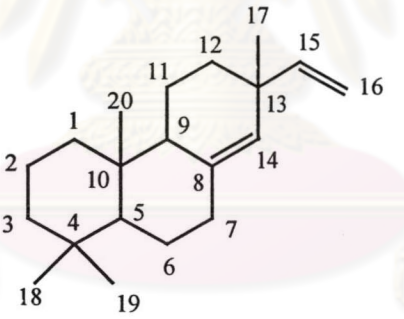

pimarane skeleton

The ^{13}C-NMR spectrum ($CDCl_3$, Figure 4) displayed twenty carbon signals which could be assigned to one carbonyl group at δ 216.8 (ketone group) and four olefinic carbons at δ 110.4 (C-16), 129.5 (C-14), 135.8 (C-8) and 148.5 (C-15). The chemical shift at δ 55.3 and 49.4 could be determined as two tertiary carbons in a cyclic skeleton (C-5 and C-9). The chemical shifts at δ 47.9, 38.1 and 37.5 were accounted for quaternary carbons. The chemical shifts of the other respective carbons could be assigned by the HSQC data (Figure 5).

Gathering from the above data, compound **1** was deduced to be 8(14),15-sandaracopimaradien-3-one. The structure is shown below.

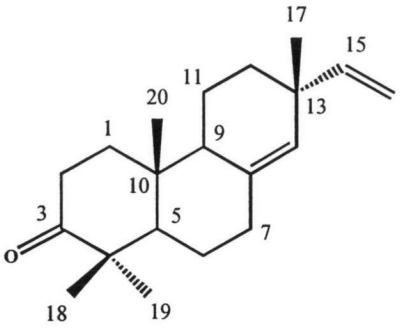

8(14),15-sandaracopimaradien-3-one

According to the reports cited in literature,[23, 33] the carbon and some proton assignments of 3-oxo-sandaracopimaradiene have not been discussed. Therefore, 2D NMR experiments were used to elucidate the structure of compound **1**.

The combination of HSQC and HMBC (Figure 6) data was indeed confirmed the pimarane skeleton having the ketone group at position 3. The C-3 showed the correlation with H-1a (2.05 ppm) and H-2 (2.67 ppm). The downfield proton signal at δ 2.67 connecting with the carbon signal at δ 34.8 was assigned for a proton at the C-2 position which clearly displayed the correlation with the δ_C 216.8 and 37.7. Therefore, the carbon chemical shift at 37.7 ppm was proposed to be C-1. The quaternary carbon at δ 47.9 was correlated with the methyl protons at δ 1.08 and 1.11. According to the pimarane skeleton, the quaternary carbon could therefore be assigned for C-4 bearing the geminal dimethyl group. The tertiary methyl proton at δ 1.08 exhibited HSQC correlation with two carbons at δ 22.3 and 26.1. The latter carbon established the correlation with H-12 and H-15; this could be concluded that these carbons were accounted for the C-19 (axial) and C-17 positions, respectively. The other methyl carbon at δ 14.7 connected with the proton at δ 1.02 could thus be assigned for C20. The assignment of other carbons and protons of compound **1** is displayed in Table 3.7. The correlation of HMBC exhibited as follows:

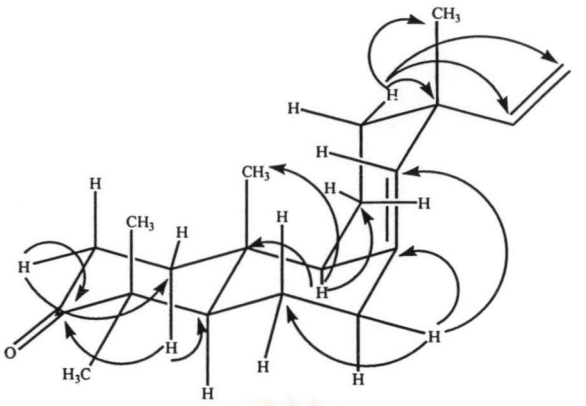

The absolute configuration was reasonably assumed to be the above structure from the value and sign of optical rotation as $[\alpha]_D = -46°$ (c, 1 in $CHCl_3$ at 23.4°C) in compound **1** and $[\alpha]_D = -56°$ (c, 2 in $CHCl_3$) for the 8(14),15-sandaracopimaradien-3-one.[23]

The ^1H, ^{13}C and 2D NMR chemical shift assignments of compound **1** are reported in Table 3.7. The structure of this compound was also confirmed by comparison the proton chemical shift of compound **1** with those of reported data of 3-oxosandaracopimaradiene.[33]

The EI mass spectrum (Figure 2) supported the proposed structure of compound **1**. The molecular ion at *m/z* 286 $[M]^+$ and other important fragmentation ion peaks at *m/z* (% relative intensity), 286 (M^+, 74.0%), 271 (100%), 258 (11.0%), 135 (66.9%) were detected. The possible mass fragmentation[34] pattern was proposed as shown in Scheme 3.2.

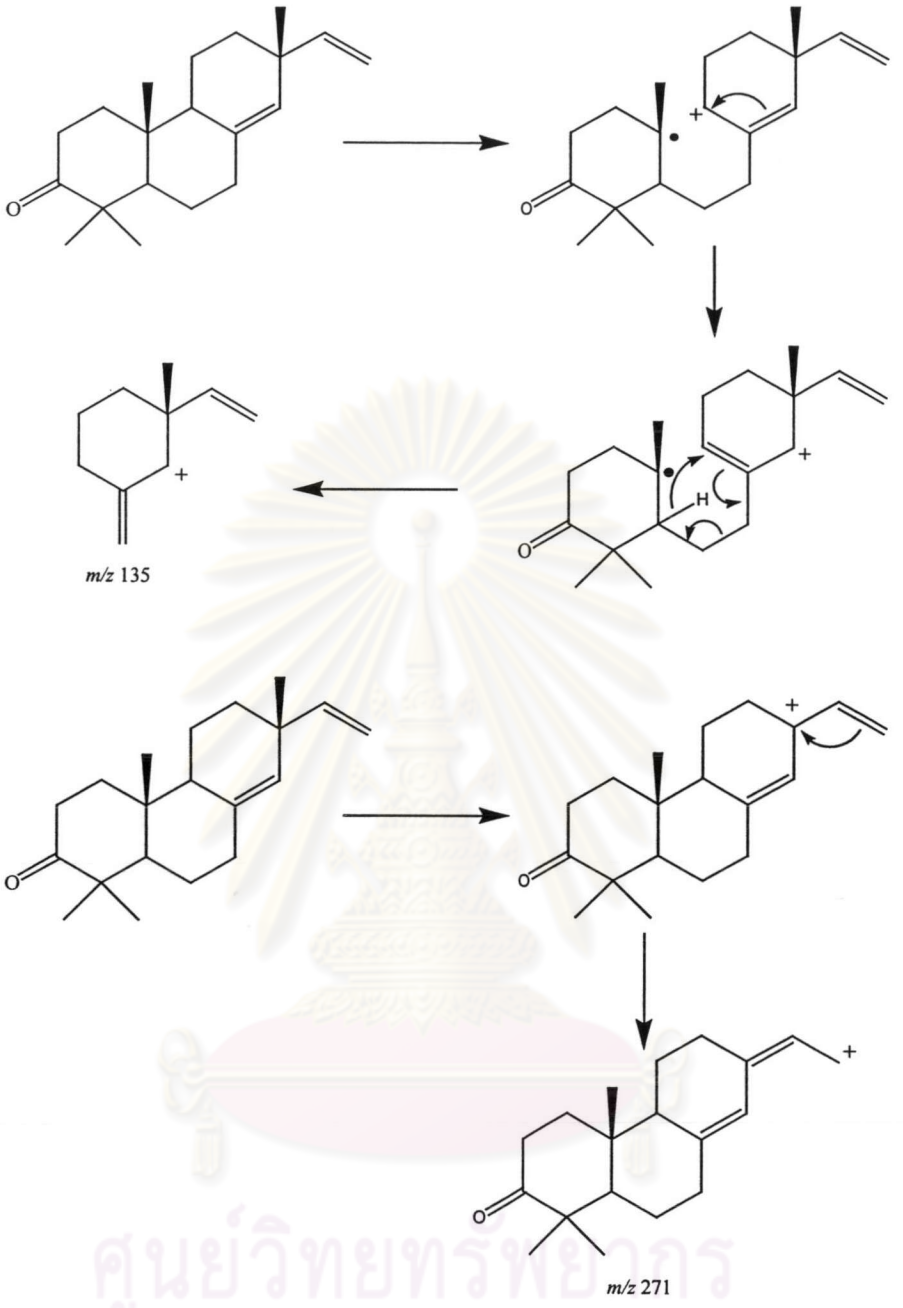

Scheme 3.2 Possible mass fragmentation pattern of compound **1**

Table 3.7 The ^{1}H, ^{13}C NMR chemical shift assignments and 2D correlation of compound **1**

Position		Chemical shift (ppm)			HMBC
		Compound **1**		3-Oxosandara copimaradiene	
		^{13}C	^{1}H	^{1}H	
1a	CH_2	37.7	2.05 (ddd, J = 13.1, 6.1, 3.5 Hz)		C2, C3, C5
1e			1.50 (m)		
2e	CH_2	34.8	2.67 (ddd, J = 3.1, 14.8, 14.8 Hz)		C1, C3
2a			2.33 (dd, J = 3.5, 18.3 Hz)		C3, C5
3	C=O	216.8			
4	C	47.9			
5	CH	55.3	1.50 (m)		
6	CH_2	23.3	1.53 (m)		
7a	CH_2	35.6	2.33 (dd, J = 4.4, 10.5 Hz)		C5, C8, C9, C14
7e			2.10 (m)		C6, C8, C14
8	C	135.8			
9	CH	49.5	1.77 (t, J = 7.9 Hz)		C8, C10, C11, C14, C20
10	C	38.1			
11	CH2	18.9	1.64 (m)		C8, C9, C13
			1.57 (m)		C7, C8, C19
12	CH2	34.4	1.50 (m)		
			1.42 (m)		C11, C13, C14, C15, C17
13	C	37.5			
14	CH	129.6	5.31 (s)	5.28	C7, C9, C12, C13,C15
15	CH	148.6	5.78 (dd, J = 17.4, 10.5 Hz)	5.80	C14, C13, C12, C17
16	CH_2	110.4	4.93 (dd, J = 17.4, 1.7 Hz)	4.91	C13, C15
			4.92 (dd, J = 10.5, 1.7 Hz)	4.90	C13, C15
17	CH_3	26.1	1.08	1.08	C1, C2, C3, C4, C5, C7, C13, C14, C15, C18
18	CH_3	25.8	1.11	1.10	C3, C4, C5, C19
19	CH_3	22.3	1.08	1.08	C1, C2, C3, C4, C5, C7, C13, C14, C15, C18
20	CH_3	14.7	1.02	1.02	C1, C5, C9, C10, C19

a: axial position, e: equatorial position

Structural elucidation of compound 2

Compound **2** had R_f 0.58 (ethyl acetate), m.p. 149-150 °C. This compound was soluble in dichloromethane, ethyl acetate and methanol, and slightly soluble in hexane.

The IR spectrum of this compound (Figure 7) gave the absorption band of hydroxyl group at 3200-3600 cm^{-1}. The characteristic absorption peak of a vinyl group was detected at 3081, 1638, 999 and 910 cm^{-1}. The C=C stretching vibration of alkene showed the absorption peak at 1638 cm^{-1}. In addition, the C-H stretching of CH_2 and CH_3 was observed at 2957 and 2871 cm^{-1}. Furthermore, the medium absorption peak of C-H asymmetric bending of geminal dimethyl appeared at 1381 cm^{-1} was also detected.

The mass spectrum (Figure 8) exhibited the molecular ion peak at *m/z* 304 [M^+] along with fragment ion peaks at *m/z* 289, 271, 255 and 121. Molecular formula was determined to be $C_{20}H_{32}O_2$ on the basis of ^1H, ^{13}C-NMR and mass spectral data.

The ^1H NMR spectrum ($CDCl_3$, Figure 9) of this compound displayed the proton signals of three tertiary methyl groups at δ 1.07 (s, CH_3), 0.97 (s, CH_3) and 0.88 (s, CH_3), an olefinic proton at δ 5.26 (s, 1H) and a vinyl proton at 5.80 (1H, dd, J = 17.6 and 10.6 Hz), 4.94 (1H, d, J = 17.6 Hz) and 4.92 (1H, dd, J = 10.6 and 1.2 Hz). The spectrum pattern was corresponded with a pimarane type skeleton containing the double bond at C8-14 and C15-16 position. The proton spectral data of compound **2** showed three methyl signals instead of usual four methyl groups associated with the pimaradiene type skeleton. The additional peak with an AB system clearly observed at 3.74 and 3.47 ppm (each doublet, J = 10.6 Hz) could be assigned to a hydroxymethyl group attached to an asymmetric center. The chemical shifts observed in the range reported for equatorial hydroxymethyl group must be at the C4 position.[35] A double doublet (J = 11.1 and 4.7 Hz) at 3.71 ppm was belonged to the proton geminal to the secondary hydroxy group.

The ^{13}C-NMR spectrum ($CDCl_3$, Figure 10) displayed twenty carbon signals which could be assigned for four olefinic carbons at δ 110.1, 129.0, 135.3 and 148.9 corresponding with C16, C14, C8 and C15, respectively, similar to those proposed in compound **1**. In addition, the carbon signals at δ 77.2 and 72.2 were attributed for primary and secondary alcohols.[35] The chemical shift at δ 50.3 and 48.6 could be possibly assigned for two tertiary carbons in a pimarane skeleton. Comparing the

carbon spectrum of this compound with that of compound **1**, the chemical shift at δ 11.0 was obviously compatible with C19. The strong shielding of the C19 methyl signal suggested its proximity to the carbon having the oxygenated function that correspondingly located at C3. The proton signal (3.71 ppm) was also in good agreement with the equatorial disposition of the OH group at C3.

Based on the above data and comparison the ^{1}H and ^{13}C-NMR with those reported in the literature,[35] the structure of compound **2** should be sandaraco pimaradiene-3β,18-diol which was previously found in the heartwood of *X. dolabriformis*.[23] The structure is shown below.

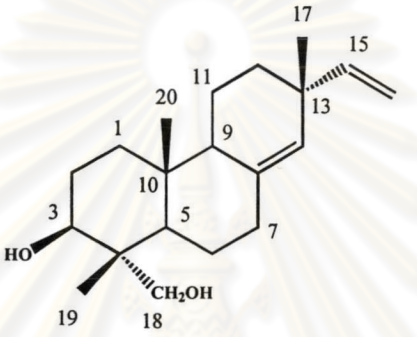

sandaracopimaradiene-3β,18-diol

Moreover, the sign of optical rotation of compound **2** as $[\alpha]_D$ = -8° (c, 0.2 in $CHCl_3$ at 23.0°C) was similar to that of 8(14),15-sandaracopimaradien-3β,18-diol as $[\alpha]_D$ = -18.5° (c, 4 in $CHCl_3$).[23] This revealed that the absolute stereochemistry of compound **2** should be similar to that of 8(14),15-sandaracopimaradien-3β,18-diol.

The ^{1}H and ^{13}C-NMR chemical shift assignments of compound **2** compared with sandaracopimaradiene-3β,18-diol[35] are presented in Table 3.8.

Table 3.8 The comparison of ^{1}H, ^{13}C NMR chemical shifts of compound **2** and sandaracopimaradiene-3β,18-diol[35]

Position	Chemical shift (ppm)			
	Compound **2**		Sandaracopimaradiene-3β,18-diol	
	^{1}H	^{13}C	^{1}H	^{13}C
1		37.0		37.4
2		27.2		27.5
3β	3.71 (dd, J = 11.1 and 4.7 Hz)	77.2	3.66 (dd, J = 10.0 and 4.2 Hz)	77.4
4		37.4		37.8
5		48.6		49.0
6		22.4		22.9
7		34.4		35.1
8		136.3		136.7
9		50.3		50.8
10		38		38.4
11		18.8		19.2
12		35.6		36.0
13		42.2		42.6
14	5.26 (s)	129	5.22 (s)	129.5
15	5.80 (dd, J = 17.6 and 10.6 Hz)	148.9	5.76 (dd, J = 17.4 and 10.7 Hz)	149.3
16	4.94 (1H, d, J = 17.6 Hz)	110.1	4.90 (dd, J = 17.4 and 1.6 Hz)	110.5
	4.92 (1H, dd, J = 10.6 and 1.2 Hz)		4.88 (dd, J = 10.7 and 1.6 Hz)	
17	0.88 (s)	26.0	0.84 (s)	26.5
18	3.74 (d, J = 10.6 Hz)	72.2	3.65 (d, J = 10.5 Hz)	71.9
	3.47 (d, J = 10.56 Hz)		3.38 (d, J = 10.5 Hz)	
19	1.07 (s)	11.5	1.03 (s)	12.0
20	0.97 (s)	15.5	0.90 (s)	15.9

The HSQC (Figure 11) and HMBC (Figure 12) experiments were performed to acquire additional information to confirm the carbon and proton assignments of compound **2**, particularly the configuration. The results revealed that the previous assignments for C17, C19 and C20 reported in the literature were different. The HSQC data clearly displayed that the methyl protons at 1.07, 0.95 and 0.87 ppm were in fact connected with the carbon at 26.0, 11.5 and 15.5 ppm, respectively. The signals of C17 and C20 appeared at almost the same location as those observed in compound **1**, the pimaradiene having the ketone group at C3, and sandaracopimaradiene,[36] the pimaradiene compound without any functional group. The comparison of chemical shifts of methyl groups is displayed in Table 3.9.

Table 3.9 The chemical shift of methyl groups of compounds **1**, **2** and sandaraco pimaradiene[36]

Position	Compound **2**		Compound **1**		Sandaracopimaradiene	
	δ_H	δ_C	δ_H	δ_C	δ_H	δ_C
17	1.07	26.0	1.08	26.1	1.02	26.0
18	-	72.2	1.11	25.8	0.87,0.78	33.8
19	0.97	11.5	1.08	22.3		22.1
20	0.88	15.5	1.02	14.7	0.85	15.0

Moreover, the previous assignment of C4 and C13, C7 and C12 was disagreed with the HMBC correlation performing in this study. The C13 exhibited the correlation with the proton connecting to C5, C18 and C19, while C4 was associated with proton connecting to C14, C15, C16 and C17. The same way, C7 was clearly correlated with C9, C14, C15 and C17, while C12 was correlated with C5, C6, C14 and C15. The correct correlation would be established if both previous carbon assignments were interchanged. The HSQC and HMBC data of compound **2** are shown in Table 3.10.

Table 3.10 The ^{1}H, ^{13}C NMR chemical shift assignments and 2D correlation of compound **2**

Position		Chemical shift (ppm)		
		^{13}C	^{1}H	HMBC
1	CH_2	37.0	1.78 (dt, J = 13.1 and 3.5 Hz)	C2, C3
			1.21 (dd, J = 13.1 and 4.4 Hz)	C17
2	CH_2	27.2	1.64 (m)	
3	CHOH	77.2	3.71 (dd, J = 11.1 and 4.7 Hz)	C2, C3, C4, C18, C19
4	C	42.2		
5	CH	48.6	1.13 (dd, J = 14.8 and 7.0 Hz)	C2, C4, C6, C7, C8, C9, C10, C18, C19, C20
6	CH_2	22.4	1.42 (m)	C5, C7, C10
7	CH_2	35.6	2.23 (dt, J = 14.0 and 3.5 Hz)	C5, C6, C8, C14
			2.06 (m)	C6, C8, C14
8	C	136.3		
9	CH	50.3	1.71 (m)	C5, C7, C8, C10, C11, C14, C17, C20
10	C	38		
11	CH_2	18.8	1.58 (m)	
12	CH_2	34.4	1.48 (m)	C9, C11
			1.37 (ddd, J = 13.1, 13.1 and 3.5 Hz)	C9, C11, C13, C15, C17
13	C	37.4		
14	CH	129	5.26 (s)	C7, C9, C12, C13
15	CH	148.9	5.80 (dd, J = 17.6 and 10.6 Hz)	C12, C13, C17
16	CH_2	110.1	4.94 (d, J = 17.6 Hz)	C13
			4.92 (dd, J = 10.6 and 1.2 Hz)	
17	CH_3	26.0	1.07 (s)	C12, C13, C14,C15
18	CH_2OH	72.2	3.74 (d, J = 10.6 Hz)	C3, C4, C5, C19
			3.47 (d, J = 10.6 Hz)	C3, C4, C18
19	CH_3	11.5	0.95 (*s*)	C3, C4, C5, C18
20	CH_3	15.5	0.87 (*s*)	C1, C5, C9, C10, C13

The mass spectrum (Figure 8) supported the proposed structure which was well-matched with the molecular ion peak, M^+, at *m/z* 304. Other important fragmentation ion peaks at *m/z* (% relative intensity): 304 (M^+, 38.9%), 289 (23.5%), 271 (38.8%), 255 (56.9%) and 121 (100%) were detected. The fragmentation pattern of this compound[34] was proposed as shown in Scheme 3.3.

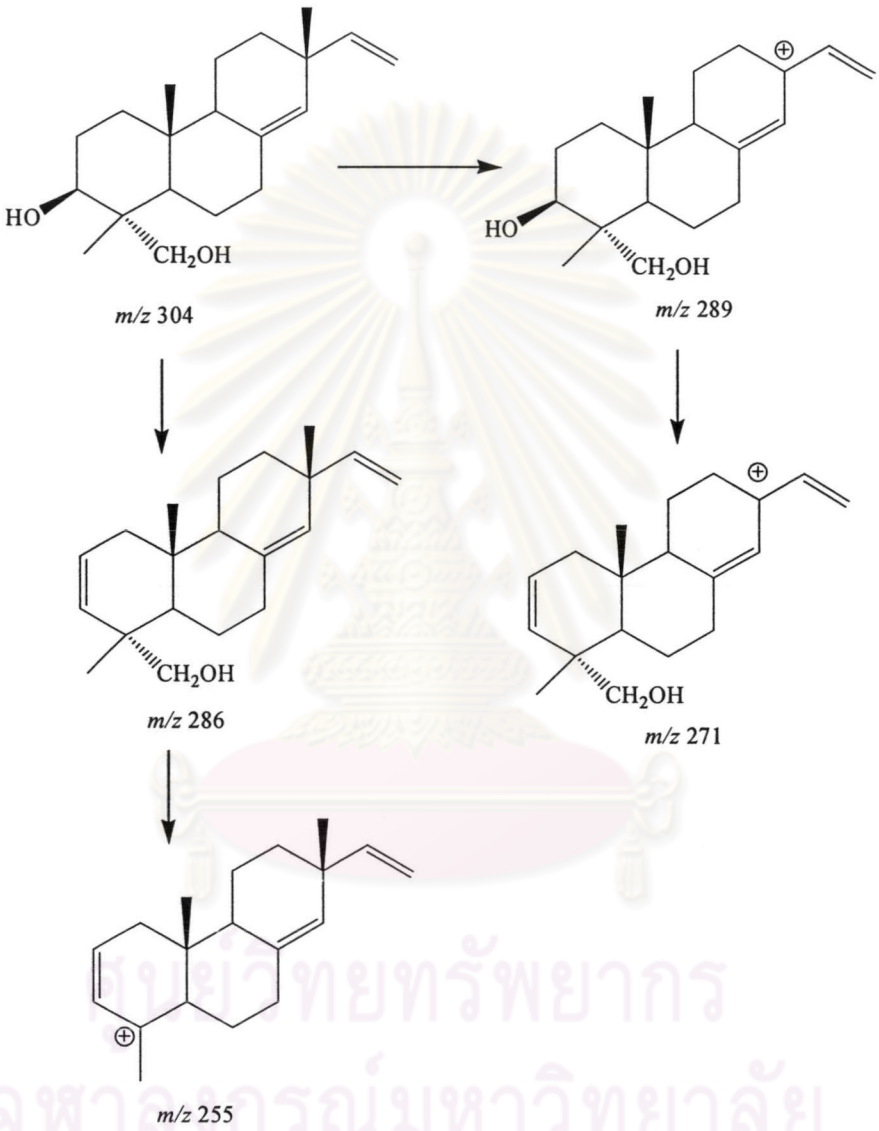

Scheme 3.3 Possible mass fragmentation pattern of compound **2**

Separation of Fraction IIA

Fraction IIA (0.52 g) was reseparated by flash column chromatography eluting with hexane to afford compound **3**. The results of separation are shown below.

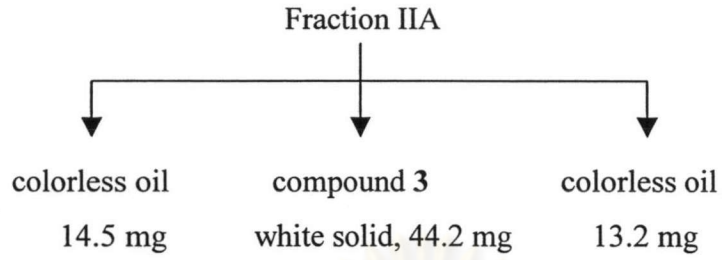

Structural elucidation of compound 3

The R_f value of compound **3** was 0.83 (hexane), m.p. 37-38 °C. This compound was soluble in hexane, dichloromethane and ethyl acetate, and slightly soluble in methanol.

The IR spectrum (Figure 13) showed the characteristic absorption peaks of a vinyl group at 3082, 1634, 996 and 910 cm^{-1}. The C=C stretching of alkene revealed an absorption peak at 1634 cm^{-1}. In addition, the C-H stretching vibration of CH_2 and CH_3 was observed at 2926 and 2854 cm^{-1}. Furthermore, the medium absorption peak of C-H asymmetric bending of geminal dimethyl appeared at 1381 cm^{-1}.

The ^1H NMR spectrum ($CDCl_3$, Figure 14) was very close to that of the pimarane type skeleton proposed for compounds **1** and **2**. The proton signals displayed four tertiary methyl groups at δ 1.06 (s, CH_3), 0.90 (s, CH_3), 0.82 (s, CH_3) and 0.87 (s, CH_3) in good agreement with those of sandaracopimaradiene presented in Table 3.9. In addition, the vinyl protons corresponded to C15-C16 position were observed at δ 5.80 (1H, dd, J = 17.6 and 10.6 Hz), 4.95 (1H, dd, J = 17.6 and 1.8 Hz) and 4.90 (1H, dd, J = 10.6 and 1.8 Hz), respectively. Besides, the olefinic proton at C8 position was appeared at δ 5.23 (s, 1H).

The ^{13}C NMR spectrum ($CDCl_3$, Figure 15) of this compound displayed twenty carbon signals corresponding to 8(14),15-pimaradiene skeleton named sandaracopimaradiene.

In addition, the sign of optical rotation of compound **3** was $[\alpha]_D$ = -7° (c, 0.5 in $CHCl_3$ at 23.0°C) similar to those of compounds **1**, **2** and 8(14),15-sandaraco pimaradiene (- *form*) as $[\alpha]_D$ = -12.4° (c, 5 in $CHCl_3$).[23] Based on the ^1H and ^{13}C

NMR spectral data and physical proporties, it could be indicated that compound **3** was (-)sandaracopimaradiene.

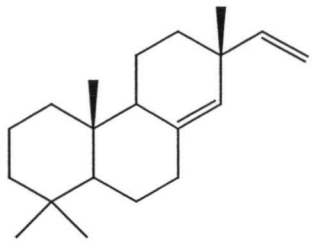

(-)sandaracopimaradiene

The structure of compound **3** was confirmed by comparison the ^{13}C NMR data with that of (-)sandaracopimaradiene. The ^{13}C NMR assignments of compound **3** and (-)sandaracopimaradiene[36] are shown in Table 3.11.

Table 3.11 The ^{13}C NMR chemical shift assignments of compound **3** and (-)sandaracopimaradiene[36]

Position	Chemical shift (ppm)	
	Compound **3**	Sandaracopimaradiene
1	39.4	39.4
2	19.6	19.1
3	42.2	42.2
4	33.3	33.3
5	54.8	54.8
6	22.6	22.6
7	36.0	36.0
8	137.3	137.3
9	50.6	50.7
10	38.3	38.3
11	18.8	18.8
12	34.6	34.6
13	37.4	37.4
14	128.3	128.5
15	149.1	149.2
16	110.0	109.9
17	26.0	26.0
18	33.8	33.8
19	22.2	22.1
20	15.0	15.0

Study on Fraction IIC

Fraction IIC was pale yellow solid showing two spots on TLC using 10% ethyl acetate in hexane as a developing solvent, after dipping with 10% H_2SO_4. The second spot (more polarity) displayed blue color identical with compound **1**.

The GCMS technique was exploited for analyzing the components in Fraction IIC. The chromatogram of Fraction IIC revealed 3 major components presented (Figure 3.1) at retention times of 33.16, 33.97 and 34.43 min corresponding with molecular ion peaks at *m/z* 272, 286 and 286, respectively. The major component was component **2** with retention time of 33.97 min. The mass spectrum of each component is exhibited in Figures 16-18, and % composition containing in this mixture is shown in Table 3.12.

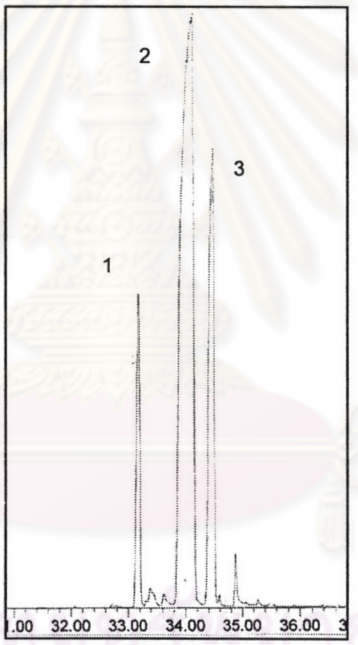

Figure 3.1 Chromatogram of Fraction IIC

Table 3.12 The composition of diterpenoids in Fraction IIC

Component	Retention time (min)	% Composition
1	33.16	9.70
2	33.97	62.27
3	34.43	21.50

The comparison of the mass spectrum of each component with Wiley 275 databases revealed that the first component with *m/z* at 272 (Figure 19) was possibly *ent*-kaur-16-ene. The second component with *m/z* at 286 (Figure 17) was equivalent to $C_{30}H_{30}O_2$ (MW 286.456). The third component, which showed *m/z* at 286 (Figure 20), was suggested to be 7,15-isopimaradiene-3-one.

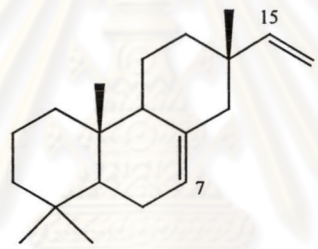

7,15-isopimaradiene

The ^{13}C NMR spectrum ($CDCl_3$, Figure 21) displayed thirty nine major carbons reasonably assigned for two sets of twenty carbons belonging to components **2** and **3**.

The high intensity signals observed at δ 148.6, 135.8, 129.6 and 110.4 belonging to the component **2** were typically vinylic and olefinic characteristic protons of 8(14),15 pimaradiene skeleton. Besides, the other carbon signals were identical with those of compound **1** presented in Table 3.13. By comparison of the carbon signals, the blue spot on TLC and the pattern of mass spectrum, it could be obviously concluded that component **2** is sandaracopimaradiene-3-one (compound **1**).

The ^{13}C NMR spectrum of the low intensity set of signals belonging to component **3** exhibited the characteristic carbon of 7,15-isopimaradiene skeleton[37] of a vinyl group at δ 109.5 and 150.0, and alkene at δ 121.2 and 135.6. In addition, the ^{13}C NMR spectrum of component **3** was directly compared with 7,15-isopimaradiene-3-one[39]

as shown in Table 3.13. The nineteen carbon signals were well identical with 7,15-isopimaradiene-3-one. However a ketone peak belonging to component **2** was only present in Fraction IIC. The absence of carbonyl carbon may due to the peak overlapped with the signal of δ 217.0 or the amount this composition was too tiny. The mass spectrum of this component was compared with that of 7,15-isopimaradiene-3-one from Wiley 275 databases as shown in Figure 20 and the possible mass fragmentation[34] is proposed in Scheme 3.4.

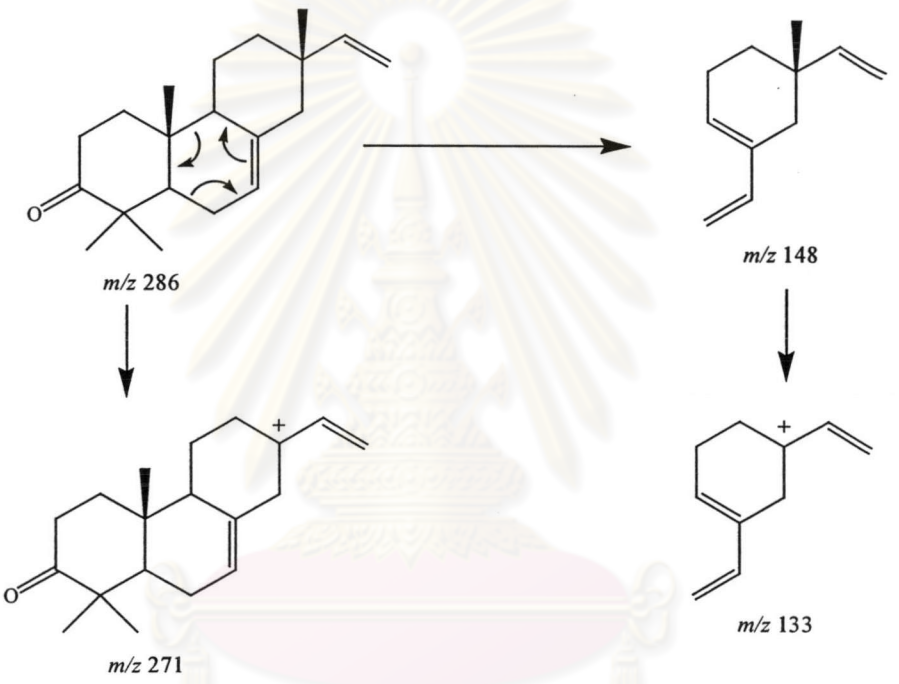

Scheme 3.4 Possible mass fragmentation pattern of component **3**

Table 3.13 The ^{13}C NMR chemical shift assignments of Fraction IIC

Position	Chemical shift (ppm)			
	Component **2**	Compound **1**	Component **3**	7,15-isopimaradiene-3-one
1	37.7	37.7	38.2	38.1
2	34.9	34.8	34.7	34.6
3	217.0	216.8	-	216.0
4	47.9	47.9	37.0	37.4
5	55.3	55.3	51.8	51.8
6	23.3	23.3	23.8	23.8
7	35.6	35.6	121.2	121.2
8	135.8	135.8	135.6	135.6
9	49.5	49.5	51.8	51.1
10	38.0	38.1	35.3	35.2
11	19.0	18.9	21.5	21.6
12	34.4	34.4	36.0	36.1
13	37.5	37.5	36.9	36.8
14	129.6	129.6	45.9	45.9
15	148.6	148.6	150.0	149.9
16	110.4	110.4	109.5	109.4
17	26.1	26.1	21.5	21.5
18	25.8	25.8	23.8	23.8
19	22.3	22.3	20.3	20.3
20	14.7	14.7	14.8	14.8

From the above data, it was lucidly seen that components **2** and **3** were compound **1** and 7,15-isopimaradiene-3-one, respectively.

Separation of Fraction IID

Fraction IID was subjected to flash column chromatography over silica gel eluting with 5% ethyl acetate in hexane. The eluting solvent was collected and then concentrated to small volume. Each fraction was monitored by TLC and similar fractions were combined. Fraction IID2 was further fractionated in the same manner. The results of separation are exhibited as follows:

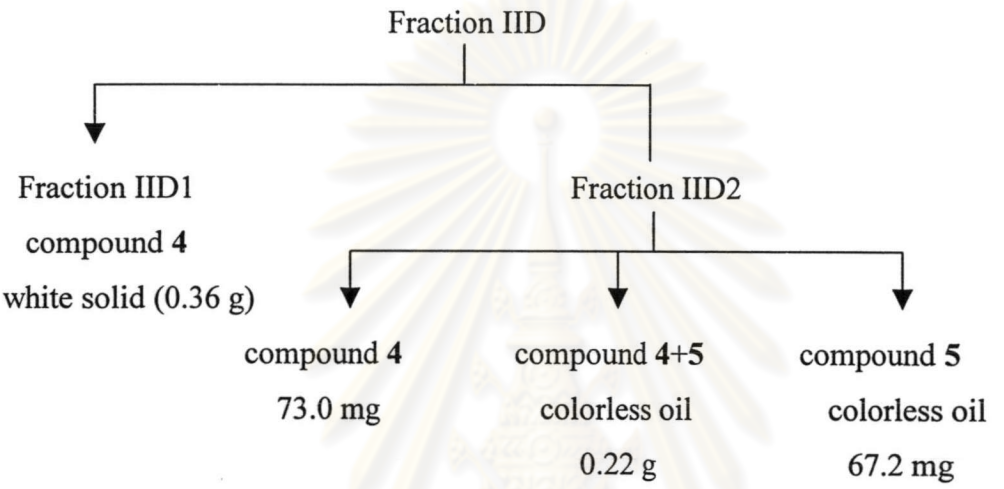

From the above scheme, compound **4** as white solid was obtained from Fraction IID. In addition, the separation of residue, Fraction IID2, led to colorless oil, compound **5**.

Structural elucidation of compound 4

The R_f value of compound **4** was 0.52 (10% ethyl acetate in hexane), m.p. 91-92 °C. In addition the optical rotation exhibited $[\alpha]_D = +46°$ (c, 1 in $CHCl_3$ at 23.5°C). This compound was soluble in hexane, dichloromethane and ethyl acetate, and slightly soluble in methanol.

The IR spectrum (Figure 22) showed the characteristic absorption peak of a carbonyl group at 1696 cm^{-1}, the C-O asymmetric stretching of ether at 1116 and 1077 cm^{-1} and a vinyl group at 3089, 1645, 995 and 910 cm^{-1}. In addition, the C-H stretching of CH_2 and CH_3 was observed at 2941 and 2867 cm^{-1}. Furthermore, the medium absorption peak of C-H asymmetric bending of geminal dimethyl was appeared at 1373 cm^{-1}.

The ^{1}H NMR spectrum ($CDCl_3$, Figure 23) of this compound displayed five tertiary methyl groups at δ 1.37 (s, CH_3), 1.33 (s, CH_3), 1.12 (s, CH_3), 1.06 (s, CH_3) and 0.94 (s, CH_3) and a typical ABX system of a vinyl proton at 5.90 (1H, dd, J = 17.6 and 10.6 Hz), 5.18 (1H, dd, J = 17.6 and 1.76 Hz) and 4.96 (1H, dd, J = 10.6 and 1.8 Hz). This proton spectral pattern was found to be close to that of labdane diterpenoid skeleton, named manoyl oxide.

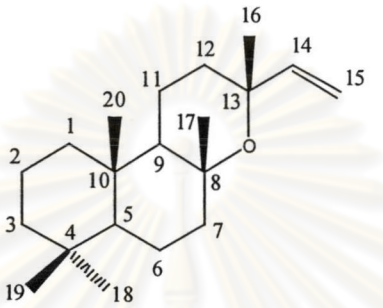

manoyl oxide

The ^{13}C-NMR spectrum ($CDCl_3$, Figure 24) displayed twenty carbon signals at δ 217.4, 147.7, 110.5, 74.8, 73.5, 55.1, 54.7, 47.4, 42.3, 37.8, 36.6, 35.9, 33.9, 28.3, 26.6, 24.9, 21.1, 20.8, 15.7 and 15.1. These characteristic carbons could be assigned to a carbonyl group at δ 217.4 (ketone group), carbons next to the ether functional group at δ 74.6 and 73.5 and two olefinic carbons at δ 110.5 (C15) and 147.6 (C14) corresponding with the manoyl oxide skeleton.

The signals at δ 2.57 (1H, ddd, J = 16.1, 10.3 and 7.6 Hz) and 2.44 (1H, ddd, J = 16.0, 7.5 and 3.9 Hz) could be assigned for the proton attached to the carbonyl carbon (CH_2C=O). The pattern of this assisted to fix the ketone group at either C1 or C3 where connecting to C2 position. Therefore, the HSQC and HMBC experiments (Figure 25 and 26, respectively) were necessary to conduct for elucidating the structure of this compound.

From HSQC data, the carbon signals at δ 15.1, 21.1, 24.9, 26.6 and 28.4 exhibited the correlation with the methyl protons at δ 0.94, 1.06, 1.37, 1.12 and 1.33, respectively. The upfield signals of proton (δ 0.94) and carbon (δ 15.1) and could be assigned for C20. The assignment of other methyl groups could be possible by the use of HMBC experiment.

The two methyl protons at δ 1.37 and 1.33 were clearly correlated with the carbon next to ether functional groups at δ 74.6 and 73.5, respectively. In addition, the chemical shift at 1.33 ppm only showed the correlation with the alkene group (C14 and C15). This demonstrated that the carbons at δ 28.4 and 24.9 should be C16 and C17, respectively. The two residue carbons at δ 21.1 and 26.6 must be placed at C18 or C19 position. Besides, these protons were correlated to the ketone group (δ 217.4). This information also supported that C3 should be a ketone carbon.

As presented above, compound **4** could be concluded as 3-oxomanoyl oxide which was previously found in the heartwood of *Xylia dolabriformis*. From the value and sign of optical rotation, comparing with the literature[23], the structure and configuration of compound **4** was shown below:

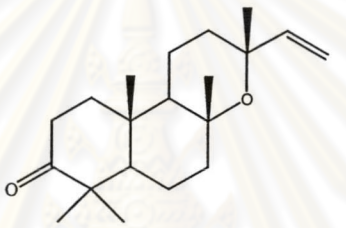

3-oxomanoyl oxide

Structural elucidation of compound 5

The R_f value of compound **5** was 0.45 (10% ethyl acetate in hexane). This compound was soluble in hexane, dichloromethane and ethyl acetate, and slightly soluble in methanol.

The ^1H NMR spectrum ($CDCl_3$, Figure 27) was identical to that of the pimarane type diterpenoid that proposed in compounds **1**, **2** and **3**. The proton signals displayed four tertiary methyl groups at δ 1.07 (s, CH_3), 1.00 (s, CH_3), 0.91 (s, CH_3) and 0.85 (s, CH_3). In addition, the vinyl proton corresponded to the C15-C16 position was observed at δ 5.81 (1H, dd, J = 17.3 and 10.4 Hz), 4.94 (1H, d, J = 17.3 Hz) and 4.91 (1H, d, J = 10.4 Hz), respectively. Besides, the olefinic proton as a sharp singlet appeared at δ 5.25 could be assigned for C14. The broad singlet at δ 3.48 was assigned to the proton on carbon attached to the secondary hydroxy group.

The ^{13}C NMR spectrum ($CDCl_3$, Figure 28) of this compound displayed twenty carbon signals which corresponded to 8(14),15-pimaradiene skeleton with 3-hydroxy group, sandaracopimaradiene-3β-ol (see also Table 3.9).

Taking into an account that the broad singlet proton at δ 3.48 was deshielded more than that noticed for sandaracopimaradiene-3β-ol (H3α at δ 3.24, dd, J = 12.3 and 4.5).[40,41] This was suggested that the C3 hydroxy group could be epimerized to the axial conformation or α-configuration. This observation was in good agreement with the fact that an axial proton in cyclohexane ring (β-ol) was more shielded than its equatorial counterpart (α-ol).[42] Compound **5** was therefore sandaracopimaradiene-3α-ol.

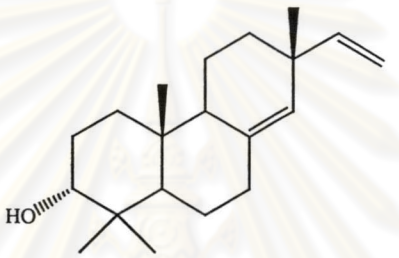

sandaracopimaradiene-3α-ol

In addition, HSQC, HMBC and COSY spectra (Figures 29-31) provided some additional information to confirm the proposed structure. Gathering from the spectroscopic data, it could be concluded that compound **5** was sandaracopimaradiene-3α-ol. The data was presented in Table 3.14.

Table 3.14 The ^{1}H, ^{13}C NMR chemical shift assignments and 2D correlation of compound **5**

Position		δ_C	δ_H	HMBC	COSY
1	CH_2	31.6	1.58 (m), 1.48 (m)	-	
2	CH_2	25.5	1.94 (m), 1.65 (m)	-	
3	CH	76.1	3.48 (br, s)	C1, C5	H2
4	C	37.5		-	
5	CH	48.2	1.5 (m)	-	
6	CH_2	22.2	1.55 (m), 1.38 (m)	-	
7a	CH_2	35.9	2.29 (m)	C6, C8, C9, C14	
7b			2.09 (m)		
8	C	137.1		-	
9	CH	50.3	1.83 (m)	C8, C10, C11, C14, C20	H14
10	C	38		-	
11	CH_2	18.7	1.55 (m), 1.39 (m)	-	
12	CH_2	34.5	1.48 (m), 1.4 (m)	-	
13	C	37.4		-	
14	CH	128.7	5.25 (s)	C7, C9, C15	H7b, H9
15	CH	149	5.81 (dd, J = 17.3, 10.4 Hz)	C12, C13, C14, C17	H16
16	CH_2	110	4.94 (d, J = 17.3 Hz), 4.91 (d, J = 10.4 Hz)	C13, C15	H15
17	CH_3	26	1.07 (s)	C12, C13, C14, C15	
18	CH_3	28.5	1.00 (s)	C3, C4, C5, C19	
19	CH_3	22.7	0.91 (s)	C3, C4, C5, C18	
20	CH_3	14.9	0.85 (s)	C1, C5, C9, C10	

The separation and structural elucidation of Fraction IIE

Fraction IIE (7.46 g) as white solid had melting range of 67-109 °C. TLC was however exhibited only one yellow purple spot after dipping with 10% H_2SO_4 in ethanol with R_f value of 0.76 (SiO_2, 20% ethyl acetate-hexane).

The ^{13}C NMR spectrum ($CDCl_3$) of this mixture (Figure 32) displayed two sets of compositions. The major composition exhibited the carbon spectra of two compounds that showed important carbon signals as follows: olefinic carbon at δ 148.9, 148.8, 137.0, 136.5, 128.8, 128.6, 110.2 and 110.0, and carbon bearing hydroxy group at δ 78.9 and 71.7. The carbon spectrum of minor composition displayed the important carbon signals as follows: olefinic carbon at δ 150.1, 135.1, 121.5 and 109.2, and carbon bearing hydroxy group at δ 79.1. These results revealed that Fraction IIE composed of at least three compounds. The characteristic carbons of two compounds in a major composition were similar to those of the pimaradiene skeleton found in compounds **1**, **2**, **3** and **5**, except for the signal belonging to a carbon attached to a hydroxy group. Besides, another compound in a minor composition revealed the same skeleton, dissimilar on the position of alkene corresponding to the 7,15-isopimaradiene skeleton.

The ^1H NMR spectrum ($CDCl_3$) of this fraction (Figure 33) showed the proton signals as follows: seven tertiary methyl groups at δ 1.04 (s, 2xCH_3), 1.01 (s, CH_3), 0.84 (s, CH_3), 0.83 (s, CH_3), 0.81 (s, CH_3) and 0.80 (s, CH_3), the proton geminal to the secondary hydroxy group (C**H**-OH) at δ 3.30 (1H, dd, J = 11.7 and 4.1 Hz), 3.41 and 3.14 (each doublet, J = 11.1 and 10.6 Hz). The chemical shift of proton confirmed that the structure of the two compounds in a major composition was belonged to 8(14),15-sandaracopimaradiene type.

The GCMS technique was employed for further analyzing the components of this mixture. The result of analysis (Figure 3.2) showed three major peaks at retention time of 24.10, 24.33 and 24.53 min. The corresponding molecular ion peaks were observed at *m/z* 288. The mass spectra of three components are displayed in Figures 34-36.

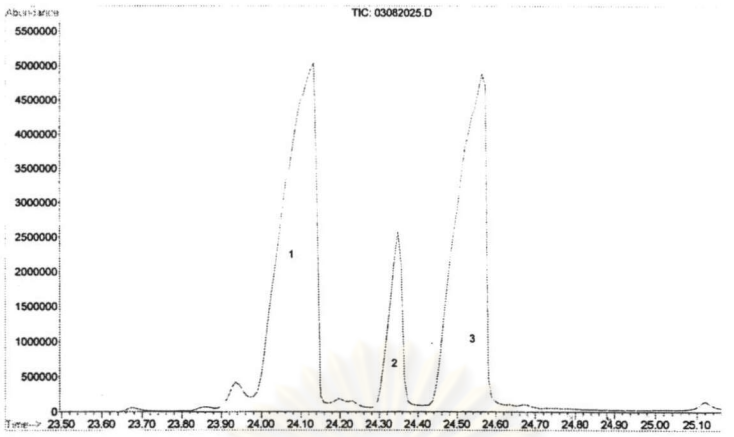

Figure 3.2 Chromatogram of Fraction IIE

The mass spectra of components **1** and **2** were compared with that of 8(14),15-isopimaradien-3β-ol and 7,15-isopimaradiene-3β-ol from Wiley 275 databases (Figures 37 and 38, respectively). The percent composition of this mixture is presented as shown in Table 3.15.

Table 3.15 The composition of diterpenoids in Fraction IIE

Component	Retention time (min)	% composition
1 (compound **6**)	24.10	45.08
2	24.33	8.33
3 (compound **7**)	24.53	40.59

As aforementioned, the structures of components **1** and **2** (in a major composition) were different in the position of an alcohol group. The spectral data implied that component **3** should be 8(14),15-isopimaradien-18-ol. The structure of this compound was confirmed by comparison of physical properties and spectroscopic data with the compound obtained from the reduction of sandaracopimaric acid (compound **9**) with $LiAlH_4$ in anhydrous ether according to the protocol described in Chapter II.

In addition, Fraction IIE was purified by crystallization with MeOH-H_2O affording compound **6** whose the structure was further elucidated.

From the spectral data and GCMS, it could be concluded that components **1**, **2** and **3** should be 8(14),15-isopimaradien-3β-ol (sandaracopimaradiene-3β-**ol**, compound **6**), 7,15-isopimaradiene-3β-ol and 8(14),15-isopimaradien-18-ol. The possible mass fragmentation[32] of components **1**, **2** and **3** is proposed as shown in Schemes 3.5-3.7.

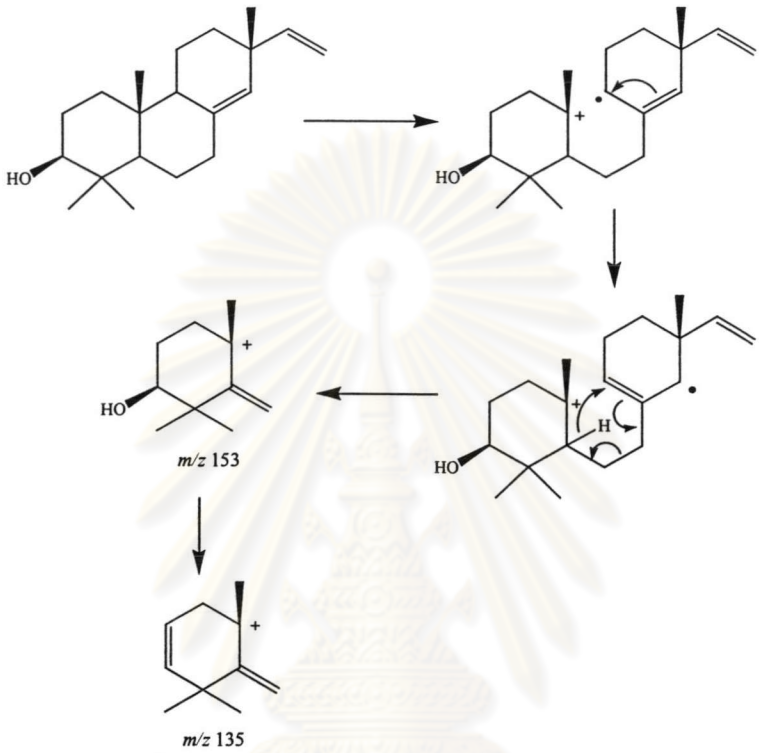

Scheme 3.5 Possible mass fragmentation pattern of component **1**

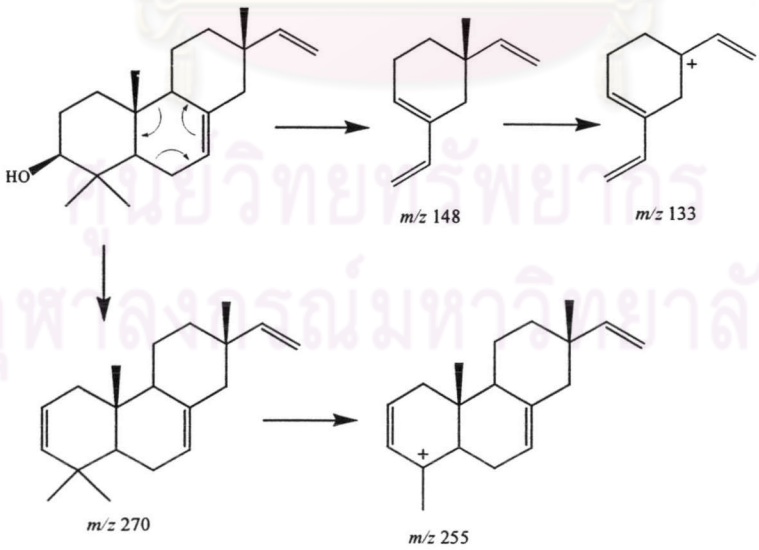

Scheme 3.6 Possible mass fragmentation pattern of component **2**

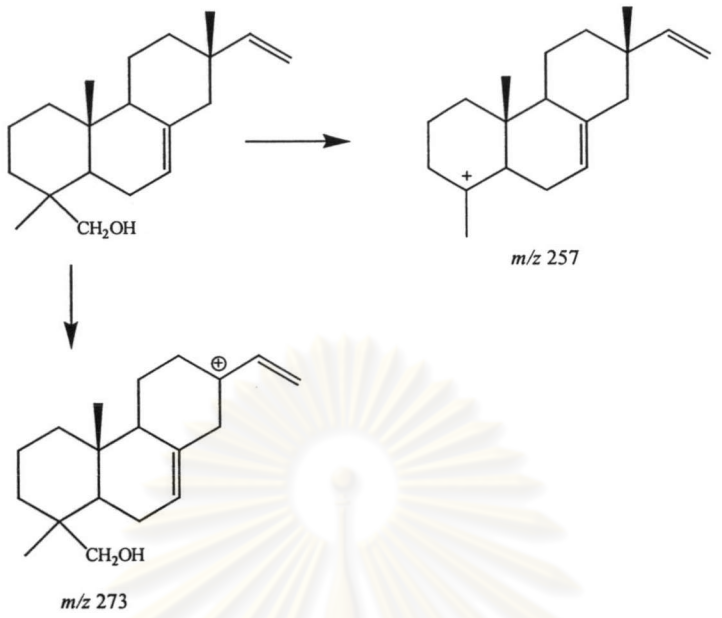

Scheme 3.7 Possible mass fragmentation pattern of component **3**

Structural elucidation of compound 6

After recrystallization of Fraction IIE with MeOH-H_2O, compound **6** was achieved as white solid (2.49 g, 6.22 %yield) and gave a single spot on TLC. The R_f value of compound **6** was 0.76 using 20% ethyl acetate in hexane as a solvent system, m.p. 126-127 °C. This compound was soluble in hexane, dichloromethane and ethyl acetate, and slightly soluble in methanol.

The IR spectrum (Figure 39) showed the characteristic absorption peaks of a vinyl group at 3082, 1634, 995 and 910 cm^{-1} and the absorption band of a hydroxyl group at 3110-3640 cm^{-1}. The C=C stretching of alkene revealed an absorption peak at 1634 cm^{-1}. In addition, the C-H stretching of CH_2 and CH_3 was observed at 2941 and 2867 cm^{-1}. Furthermore, the absorption peak of C-H asymmetric bending of geminal dimethyl appeared at 1377 cm^{-1}.

The ^{1}H-NMR spectrum ($CDCl_3$, Figure 40) displayed typical proton signals of pimarane type diterpenoids. The presence of four tertiary methyl groups was manifestly detected at δ 1.07 (s, CH_3), 1.04 (s, CH_3), 0.86 (s, CH_3) and 0.83 (s, CH_3), a vinyl proton as ABX system at δ 5.80 (1H, dd, J = 17.6 and 10.6 Hz), 4.92 (1H, d, J = 17.6 and 1.8 Hz) and 4.94 (1H, d, J = 10.6 and 1.8 Hz) and an olefinic proton as a sharp singlet at δ

5.27. In addition, the proton on carbon connecting to the secondary hydroxyl group as a double doublet (J = 11.7 and 4.1 Hz) centered at δ 3.30, in agreement with the range of signal reported for an axial proton at 3 position.[40,41]

The ^{13}C-NMR spectrum ($CDCl_3$, Figure 41) displayed twenty carbon signals corresponded with 8(14),15-pimaradiene skeleton. Four olefinic carbons could be observed at δ 110.0, 128.8, 136.7 and 149.0 associated with C16, C14, C8 and C15, respectively. In addition, one carbinol was found at δ 79.2. The chemical shift at δ 54.1 and 50.4 could be assigned for two tertiary carbons. On the basis of spectroscopic data and a comparison of the ^{13}C-NMR spectrum of compound **6** with published data (shown in Table 3.16), the structure of this compound was elucidated as sandaracopimaradiene-3β-ol.[40,41]

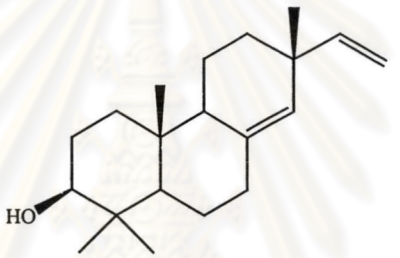

sandaracopimaradiene-3β-ol

In addition, the sign and optical rotation value of compound **6** as $[\alpha]_D$ = -18° (c, 1 in $CHCl_3$ at 22.6°C) was in good agreement with sandaracopimaradiene-3β-ol as $[\alpha]_D$ = -19.5° (c, 5 in $CHCl_3$).[23]

This structure was confirmed by comparing physical properties and spectroscopic evidence with the compound derived from the reduction of compound **1** with $NaBH_4$ according to the procedure cited in Chapter II. The ^{1}H-NMR spectrum (Figure 42) of the reduction product was identical with that of compound **6**. Based on the above physical properties and spectroscopic data, it could be concluded that this product and compound **6** is sandaracopimaradiene-3β-ol.

HSQC, HMBC and COSY (Figures 43-45) were conducted to gain additional information for confirming the proposed structure. The data obtained was ascertained for the proposed structure and the proton and carbon chemical shift assignments are shown in Table 3.16.

Table 3.16 The ^{1}H, ^{13}C NMR chemical shift assignments and 2D correlation of compound **6** comparing with sandaracopimaradiene-3β-ol

Position		δC		δH	HMBC	COSY
		Cpd 6	Sandaracopimaradiene-3β-ol	Cpd 6		
1	CH_2	37.3	37.3	1.88 (dt, *J* = 12.9 and 3.5 Hz)	C2	
				1.20 (dd, *J* = 13.5, 13.5 and 3.5 Hz)	C2	
2	CH_2	27.6	27.7	1.67 (m), 1.59 (m)	-	
3	CH	79.2	79.1	3.30 (dd, *J* = 11.7 and 4.1 Hz)	C18, C19	
4	C	39.0	39.0	-	-	
5	CH	54.1	54.2	1.06 (m)	-	
6	CH_2	22.2	22.3	1.62 (m), 1.38 (m)	-	
7	CH_2	35.9	35.9	2.31 (ddd, *J* = 14.1, 4.7 and 2.4 Hz)	C5, C8, C9, C14	H6
				2.07 (m)	C6, C8, C14	
8	C	136.7	136.6	-	-	
9	CH	50.4	50.4	1.70 (m)	-	
10	C	38.1	38.2	-	-	
11	CH_2	18.8	18.8	1.60 (m)	-	H6
12	CH_2	34.5	34.6	1.48 (m)	C9, C11	
				1.38 (m)	C5, C7, C9, C10, C11	
13	C	37.5	37.5	-	-	
14	CH	128.8	128.9	5.27 (s)	C7, C9, C12, C13, C15	
15	CH	149.0	148.9	5.80 (dd, *J* = 17.6 and 10.6 Hz)	C13, C14, C17	
16	CH_2	110.0	110.1	4.94 (dd, *J* = 17.6, 1.8 Hz), 4.92 (dd, *J* = 10.6, 1.8 Hz)	C13, C15	
17	CH_3	26.0	26.0	1.07 (s)	C12, C13, C14, C15	
18	CH_3	28.5	28.5	1.04 (s)	C3, C4, C5, C19	H7
19	CH_3	15.8	15.7	0.86 (s)	C3, C4, C5, C18	
20	CH_3	15.0	15.0	0.83 (s)	C1, C5, C9, C10, C13	

Structural elucidation of compound 7

Compound **7**, constituting as a major composition of Fraction IIE, was confirmed the structure by comparing with the product obtained from the reduction of sandaracopimaric acid (compound **9**) with $LiAlH_4$ in anhydrous ether according to that described in Chapter II.

The reduction product or compound **7** had R_f value as 0.76 using 20% ethyl acetate in hexane as a solvent system. This compound was soluble in hexane, dichloromethane and ethyl acetate and slightly soluble in methanol.

The ^{1}H-NMR spectrum ($CDCl_3$, Figure 46) showed three methyl signals instead of the usual four methyl groups at δ 1.04 (s, CH_3), 0.84 (s, CH_3) and 0.81 (s, CH_3), associated with a pimarane type skeleton. A methyl group had therefore been replaced by a hydroxymethyl group which appeared as an AB system at δ 3.40 and 3.13 (each doublet, J = 10.9 Hz) identical with the carbinol proton appeared from Fraction IE. The signals of this methylene group attached to a hydroxy was in good agreement with that reported[36,43] for an equatorial conformation (C18) which was the same as the position of carboxylic acid (compound **9**). The obtained information established the presence of an olefinic proton as a sharp singlet at δ 5.21 and the vinyl proton at δ 5.78 (1H, dd, J = 17.9 and 10.9 Hz), 4.92 (1H, dd, J = 17.9 and 1.6 Hz) and 4.88 (1H, dd, J = 10.9 and 1.6 Hz).

The ^{13}C-NMR spectrum ($CDCl_3$, Figure 47) displayed twenty carbon signals corresponded with 8(14),15-pimaradiene skeleton. Four olefinic carbons could be observed at δ 110.0, 128.7, 137.0 and 149.1 associated with C16, C14, C8 and C15, respectively. The chemical shift at δ 72.2 was assigned to be carbinol exchanged from the carboxylic carbon of compound **9** (185.4 ppm). The other carbon signals were also corresponded with those of compound **9**. Gathering from the above results, this product is no doubt sandaracopimaradiene-18-ol. This implied that compound **7** is also 8(14),15-isopimaradiene-18-ol (sandaracopimaradiene-18-ol).

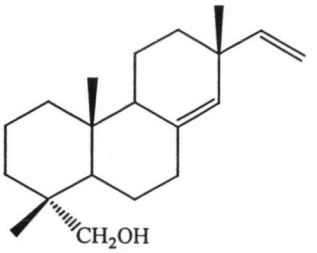

sandaracopimaradiene-18-ol

The HSQC and HMBC spectra (Figures 48 and 49) were useful for the assignment of this product and confirming the proposed structure. The carbon and proton assignments of this product are shown in Table 3.17.

Table 3.17 The ^{1}H, ^{13}C NMR chemical shift assignments and 2D correlation of the product obtained from the reduction of compound **9**

Position		Chemical shift (ppm)		HMBC
		^{13}C	^{1}H	
1	CH_2	38.9	0.89 (m)	
			1.72 (m)	
2	CH_2	18.4	1.60 (m)	
3	CH_2	35.5	1.41 (m), 1.30 (m)	
4	C	38.2		
5	CH	47.9	1.34 (m)	
6	CH_2	22.4	1.55 (m), 1.30 (m)	
7	CH_2	35.7	2.24 (m)	C5, C6, C8, C14
			2.08 (m)	C6, C8, C14
8	C	137.0		
9	CH	50.6	1.77 (t, J = 7.8 Hz)	
10	C	37.8		
11	CH_2	18.8	1.60 (m)	
12	CH_2	34.6	1.35 (m)	
13	C	37.4		
14	CH	128.7	5.21 (s)	C7, C9, C12, C13, C15
15	CH	149.1	5.78 (dd, J = 17.9 and 10.9 Hz)	C12, C13, C17
16	CH_2	110.0	4.92 (dd, J = 17.9 and 1.6 Hz)	
			4.88 (dd, J = 10.9 and 1.6 Hz)	C13, C15
17	CH_3	26.0	1.04 (s)	C12, C13, C14,C15
18	CH_2OH	72.2	3.40 (d, J = 10.9 Hz)	C3, C4, C5, C19
			3.13 (d, J = 10.9 Hz)	
19	CH_3	18.0	0.81 (s)	C3, C4, C5, C10, C18
20	CH_3	15.6	0.84 (s)	C1, C4, C5, C9, C13

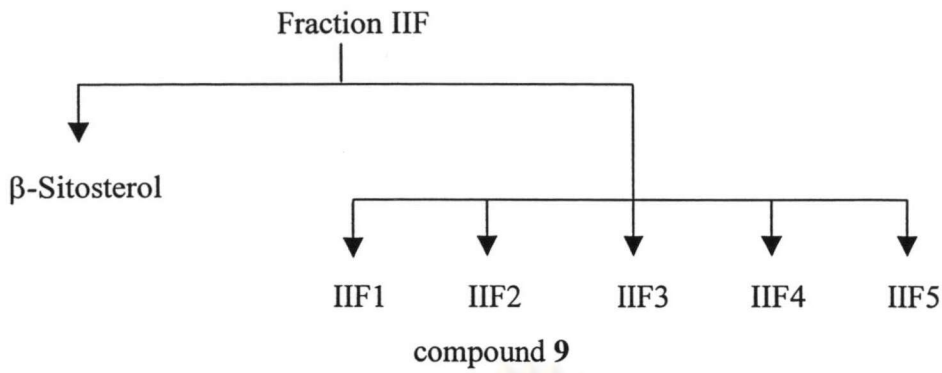

Scheme 3.8 The separation of the residue Fraction IIF

Further purification of Fraction IIF2 by recrystallization with acetone yielding needle crystal (0.2 g, 0.625% yield) as compound **9**. In addition, Fraction IIF3 was first purified by flash column chromatography eluting with 5% ethyl acetate in hexane and then the receiving solid was further purified by recrystallization with acetone to yield compound **9** (54.3 mg).

Structural elucidation of compound 9

Compound **9** had R_f 0.71 (20% ethyl acetate in hexane), m.p. 168.5-169.4°C. This compound was soluble in dichloromethane, ethyl acetate and slightly soluble in hexane, acetone and methanol.

The IR spectrum of this compound (Figure 50) displayed the absorption band of a hydroxyl group at 3200-3700 cm^{-1}, a carbonyl group at 1696 cm^{-1} (C=O) and a vinyl group at 3073, 1638, 995 and 910 cm^{-1}. In addition, the C-H asymmetric bending of CH_2 and CH_3 was observed at 1400-1500 cm^{-1}.

The ^1H NMR spectrum ($CDCl_3$) of this compound (Figure 51) displayed the protons of three tertiary methyl groups at δ 1.25 (s, CH_3), 1.04 (s, CH_3) and 0.84 (s, CH_3) indicating that one methyl group was replaced with a carboxylic group. The carboxylic group was assigned to locate at C18 position from the chemical shift of C20 (0.84 ppm) based upon the previous data reported.[44] In addition, the proton at C5 (1.92 ppm) of this compound was deshielded comparing with those reported in compounds **1**, **2**, **5** and **6**. This implied that the carboxylic group should be placed in C18 position. The typical signal of 8(14),15-pimaradiene established vinyl protons at δ 5.77 (1H, dd, J = 17.1 and

10.2 Hz), 4.91 (1H, d, J = 17.1 Hz) and 4.88 (1H, d, J = 10.2 Hz), and an olefinic proton at δ 5.22 (s, 1H).

The ^{13}C NMR spectrum ($CDCl_3$) of this compound (Figure 52) displayed twenty carbon signals corresponded with a pimarane skeleton. The important signal of carboxylic carbon was viewed at δ 185.4. Other signals were detected and compared with the reported sandaracopimaric acid[44] as presented in Table 3.17.

In addition, the sign of optical rotation in compound **9** as $[\alpha]_D$ = -7° (c, 0.5 in $CHCl_3$ at 23.0°C) was similar with those of compounds **1**, **2** and 8(14),15-sandaraco pimaradiene (- *form*) as $[\alpha]_D$ = -12.4° (c, 5 in $CHCl_3$).[23] Based on the ^1H and ^{13}C NMR and physical proporties, it could be indicated that compound **9** was (-)sandaracopimaric acid.

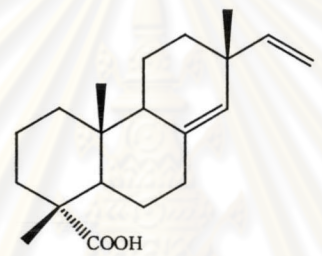

(-)sandaracopimaric acid

HSQC, HMBC and COSY (Figure 53, 54 and 55, respectively) spectra provided an additional information to endorse the proposed structure. The carbon and proton assignments of compound **9** compared with sandaracopimaric acid are shown in Table 3.19.

Moreover, the structure of compound **9** was also confirmed by single crystal X-ray diffraction analysis.[45] Single crystal of this compound was prepared by carefully recrystallization with acetone. The computer-generated ORTEP drawing and a plot of crystal packing of compound **9** are shown in Figure 3.3.

Table 3.19 The ^{1}H, ^{13}C NMR chemical shift assignments and 2D correlation of compound **9** comparing with the sandaracopimaric acid

Position		δC		δH	HMBC	COSY
		Cpd 9	sandaracopimaric acid	Cpd 9		
1	CH_2	38.3	38.4	1.74 (m)	-	
				1.14 (m)	C2, C20	
2	CH_2	18.1	18.3	1.54 (m)	-	
3	CH	37.0	37.1	1.78 (m)	-	
				1.62 (m)	C1, C2, C4, C5	
4	C	47.3	47.2		-	
5	CH	48.8	48.7	1.92 (dd, J = 12.3 and 2.1 Hz)	C4, C6, C7, C9, C10, C18, C19, C20	H6 (1.46)
6	CH_2	24.9	24.9	1.46 (m)	-	
				1.27 (m)	C7, C8	
7	CH_2	35.5	35.5	2.22 (dd, J = 13.9, 2.7 Hz)	C4, C5, C6, C8, C9, C14	
				2.12 (ddd, J = 13.9, 13.9, 5.4 Hz)	C6, C8, C14	H6
8	C	136.6	136.2		-	
9	CH	50.5	50.7	1.81 (m)	C8, C10, C14, C20	
10	C	37.7	37.8		-	
11	CH_2	18.5	18.8	1.54 (m)	-	
12	CH_2	34.4	34.6	1.39 (m)	-	
13	C	37.4	37.4		-	
14	CH	129.1	129.3	5.22 (s)	C7, C9, C13, C15, C17	H7 (2.12)
15	CH	148.9	149.0	5.77(dd, J = 17.1, 10.2 Hz)	C14, C13, C12, C17	
16	CH_2	110.2	110.5	4.91(d, J = 17.1 Hz), 4.88 (d, J = 10.2 Hz)	C13, C15	
17	CH_3	26.0	26.2	1.04 (s)	C12, C13, C14, C15, C16	
18	C	185.4	185.3			
19	CH_3	16.8	16.8	1.25 (s)	C3, C4, C5, C18	
20	CH_3	15.2	15.3	0.84 (s)	C1, C5, C9, C10	

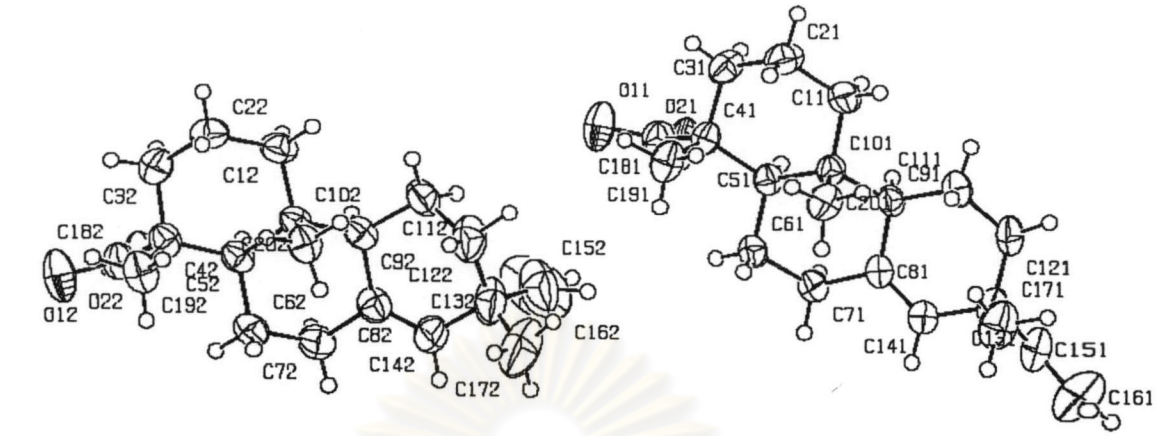

(a)

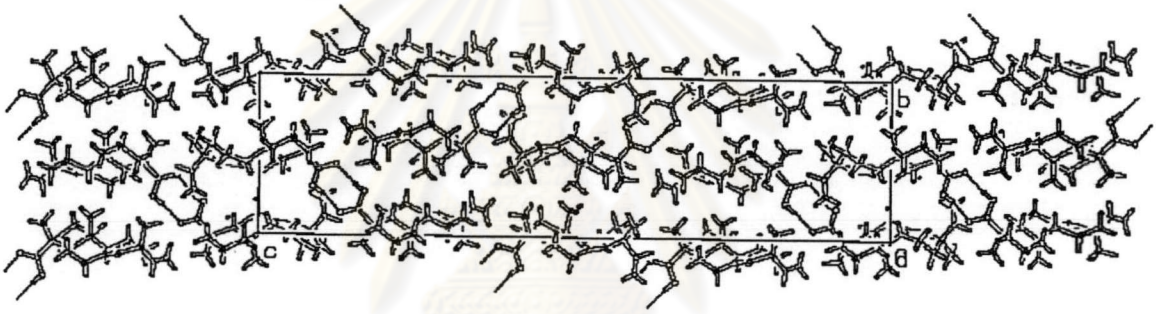

(b)

Figure 3.3 a) The computer-generated ORTEP drawing of compound **9** and b) A plot of crystal packing of compound **9**

In summary, nine compounds could be isolated from Fractions IIA-IIG. Sandaracopimaradiene (**3**, 44.2 mg) and sandaracopimaradien-3β,18-diol (**2**, 0.69 g) were obtained from Fractions IIA and IIG, respectively. Sandaracopimaradien-3-one (**1**, 6.5 g), the major compound of this extract, was fruitfully isolated from both Fractions IIB and IIC. 3-Oxomanoyl oxide (**4**, 0.43 g) and sandaracopimaradien-3α-ol (**5**, 67.2 mg) were isolated from Fraction IID. Sandaracopimaradien-3β-ol (**6**, 2.49 g) and sandaraco pimaradien-18-ol (**7**) were derived from Fraction IIE. While, β-sitosterol (**8**, 18.2 mg) and sandaracopimaradien-18-oic acid (**9**, 0.25 g) were obtained from Fraction IIF. The isolation diagram of all substances was summarized in Scheme 3.9.

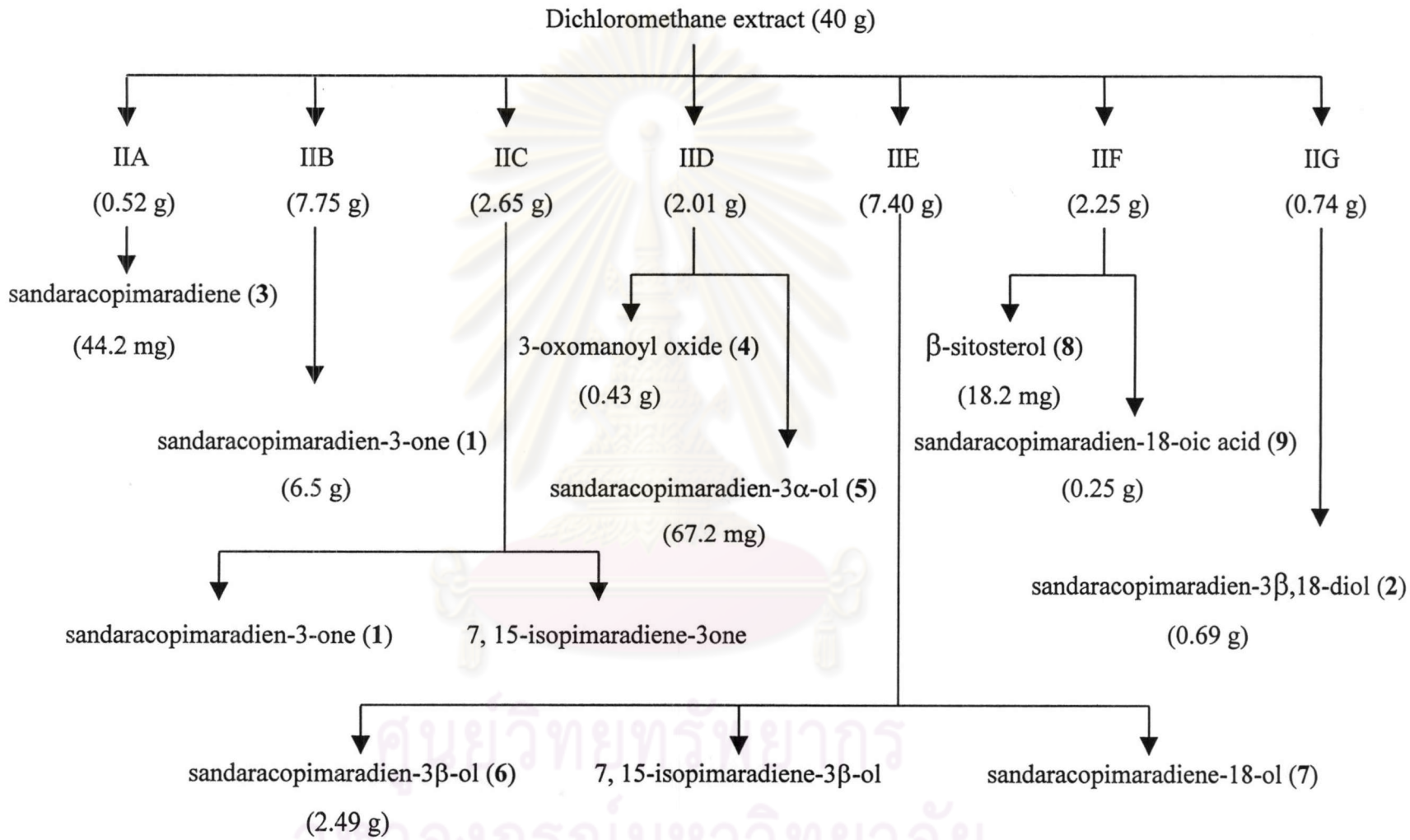

Scheme 3.9 Isolation diagram of the dichloromethane extract from the heartwood of *X. xylocarpa*

3.6 The results of biological activity of the isolated compounds

As mentioned above, the separation of dichloromethane extract from *X. xylocarpa* led to the isolation of eight substances. The isolated substances, except compound **5**, were further studied for biological activity. The antifeedant activity against *S. litura* and termite including phytoxicity against lettuce seedling were selected for exploration followed the protocols described in Chapter II.

3.6.1 The results of antifeedant activity against *S. litura*

Seven isolated compounds were evaluated for the antifeedant activity against *S. litura* by choice leaf disk bioassay. The results of antifeedant activity (%) are displayed in Table 3.20.

Table 3.20 The antifeedant acitvity (%) against *S. litura* of the isolated compounds

Compound	Antifeedant activity (%)			
	0.125 mg/disk	0.25 mg/disk	0.5 mg/disk	1.0 mg/disk
1	-	-	10.90 (± 9.4)	27.83 (± 14.0)
2	-	-	0.56 (± 13.6)	24.53 (± 2.1)
3	-	-	6.78 (± 6.6)	-
4	-	43.64 (± 12.8)	46.85 (± 10.2)	41.97 (± 6.2)
6	-	-	-	-15.43 (± 9.0)
7	-	-	-	2.91 (± 2.0)
9	26.34 (± 5.7)	60.71 (± 4.7)	71.85 (± 3.9)	81.58 (± 1.6)

From the results, compound **9** (sandaracopimaric acid) revealed the highest activity while compound **4** (3-oxomanoyl oxide) exhibited medium activity. Compounds **1** (sandaracopimaradiene-3-one), **2** (sandaracopimaradiene-3,18-diol) and **3** (sandaraco pimaradiene) displayed low activity whereas compounds **6** (sandaracopimaradiene-3β-ol) and **7** (sandaracopimaradiene-18-ol) were inactive. Calculating by Probit analysis program, the ED_{50} of compound **9** is 2.75×10^{-7} mol/cm^2 that showed comparatively potent to the commercial substance, rotenone[14] ($ED_{50} = 1.5 \times 10^{-7}$ mol/cm^2).

As the comparison with preliminary result of dichloromethane crude extract, it could be concluded that one of the active principles should be compound **9** and/or

compound **4**. The carboxylic group at C4 is indeed virtually essential for the antifeedant acitivity against *S. litura*.

3.6.2 The results of antifeedant activity against termite

The seven isolated substances were also tested for the antifeedant activity against termite by bioassay described in Chapter II. The results of antifeedant activity (%) are displayed in Table 3.21.

Table 3.21 The antifeedant activity (%) against termite of the isolated compounds

Compound	Antifeedant activity (%)			
	5 μg/disk	10 μg/disk	50 μg/disk	100 μg/disk
1	-	39.8 (± 14.7)	97.5 (± 2.0)	97.9 (± 1.7)
2	65.4 (± 7.2)	79.1 (± 18.2)	-	99.0 (± 0.6)
3	-	9.8 (± 7.8)	84.2 (± 6.2)	79.7 (± 11.7)
4	96.5 (± 1.6)	97.3 (± 2.2)	-	97.3 (± 0.5)
6	47.1 (± 0.9)	97.4 (± 0.7)	-	82.8 (± 12.8)
7	35.6 (± 13.1)	98.9 (± 0.4)	-	96.4 (± 2.8)
9	-	-	91.6 (± 1.2)	93.2 (± 2.9)

According to the above results, the entire isolated compounds exhibited excellent feeding inhibition, especially compound **4** showed 96.5% feeding inhibition at 5 μg/disk, while compounds **2**, **6**, **7** and **9** exhibited less activity than compound **4**.

This result strongly indicated that the isolated compounds from the heartwood of *X. xylocarpa* had potential for feeding inhibition against termite.

3.6.3 The results of phytotoxicity against lettuce seedling

The phytotoxicity was chosen for checking the toxicity of substances in crops. The effect of isolated substances on the growth seedlings against lettuce was evaluated according to the procedure written in Chapter II, and the results are demonstrated in Table 3.22.

Table 3.22 Effect of isolated substances on the growth of seedlings

Compound	Conc. (ppm)	Plant growth rate (%)			F.W
		Cotyledon	Hypocotyl	Radicle	
1	500	87.3 (± 0.23)	110.9 (± 0.05)	154.3 (± 1.46)	85.5
	100	91.3 (± 0.27)	95.7 (± 0.04)	115.2 (± 0.88)	77.7
2	500	86.1 (± 0.21)	93.6 (± 0.04)	265.4 (± 1.29)	79.7
	100	94.9 (± 0.27)	100.0 (± 0.05)	188.4 (± 0.66)	78.1
3	500	99.0 (± 0.18)	91.5 (± 0.04)	145.3 (± 1.11)	101.5
	100	100.4 (± 0.17)	95.7 (± 0.04)	99.4 (± 0.42)	96.5
4	500	82.3 (± 0.20)	93.5 (± 0.04)	166.3 (± 0.73)	74.5
	100	91.7 (± 0.19)	104.3 (± 0.05)	135.8 (± 0.63)	94.5
6	500	100.0 (± 0.21)	97.9 (± 0.05)	125.9 (± 0.53)	94.0
	100	110.6 (± 0.29)	102.1 (± 0.05)	163.1 (± 1.39)	96.2
7	500	100.4 (± 0.18)	104.3 (± 0.05)	203.5 (± 1.11)	89.4
	100	101.1 (± 0.21)	102.1 (± 0.05)	165.4 (± 1.67)	94.8
9	500	104.4 (± 0.19)	89.4 (± 0.03)	148.5 (± 1.47)	83.6
	100	112.1 (± 0.22)	93.6 (± 0.04)	108.7 (± 0.84)	103.1

In this experiment the doses applied were 500 and 100 ppm. All of isolated compounds did not reveal the effect on the growth of lettuce seedling. This pointed out that the isolated substances might be used as environmental friendly insect antifeedant.

3.7 Review of pimarane type diterpenoid

The diterpenes are C_{20} compounds that are widely distributed in plant and fungal origin. They usually occur as mixtures of closely related compounds. Pimarane derivatives are a group of tricyclic diterpenoid which have been found in various plants and fungi that exhibited some biological activities.[46] Some of these pimarane derivatives are exemplified as follows:

Recently, several pimaric acid derivatives, including pimaric and isopimaric acids, abundant in pine rosin exhibited novel potent BK_{ca}, large conductance Ca^{2+}-dependent K^+, channel opener.[47,48] In addition, fermentation broth of an unidentified

coelomycete produced a diol, maxikdiol, which was a powerful agonist of the maxi-K channel.[49]

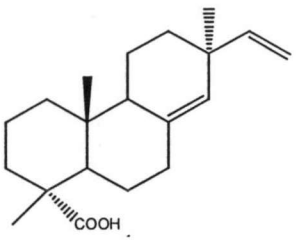

pimaric acid

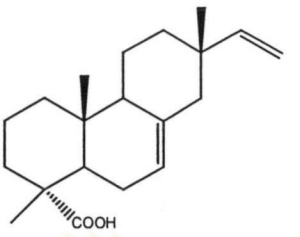

isopimaric acid

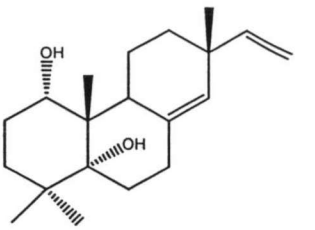

maxikdiol

As seen from the above related structures, sandaracopimaric acid (found in this research as compound **9**) has been identified as the lipoxygenase inhibitor from *Juniperus phenicea*.[45] 7β-Hydroxysandaracopimaric acid was also obtained from the roots of *Juniperus chinensis*.[50]

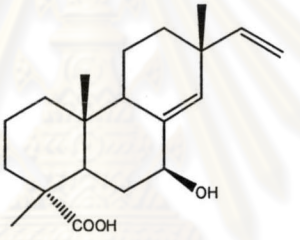

7β-hydroxysandaracopimaric acid

Some other pimaranes have been addressed as phytotoxins such as sphaeropsidin A from the cypress canker fungus *Sphaeropsis sapinea* var. *cupressi*.[51]

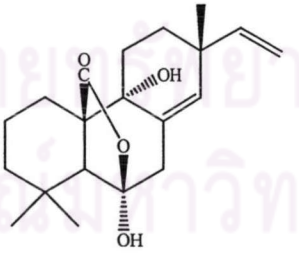

sphaeropsidin A

A number of pimarane derivatives have been isolated from Labiatae family. For example, two highly oxygenated pimaranes, orthosiphols A and B, were obtained from the leaves of the medicinal plant *Orthosiphon stamineus* and exhibited potent inhibitory activity against the inflammation induced by the tumour promoter 12-*O*-

tetradecanoylphorbol-13-acetate.[52,53] 7α,18-Dihydrosandaracopimaradiene which possessed antimicrobial and antispasmodic properties have been isolated from an important medicinal plant in Central Africa *Iboza riparia*.[54]

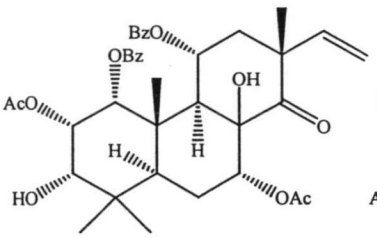

orthosiphol A

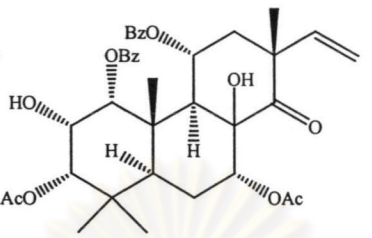

orthosiphol B

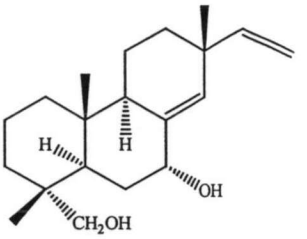

7α,18-Dihydrosandaracopimaradiene

A number of pimarane has also been isolated from the Zingiberaceae such as sandaracopimaradienes oxygenated at C1 and C9, *e.g.* (**10**) have been obtained from the rhizomes of a Thai *Kaempferia* species.[55]

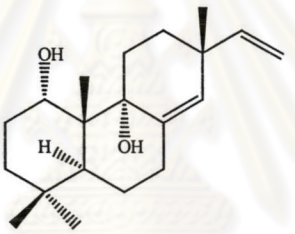

10

A large number of diterpenoid phytoalexins (*ent*-pimarane derivatives) such as oryzalexins E,[56] F[57] and *ent*-isopimara-8(14),15-dien-3β-ol,[41] have been detected in rice *Oryza sativa* infected with various fungi.

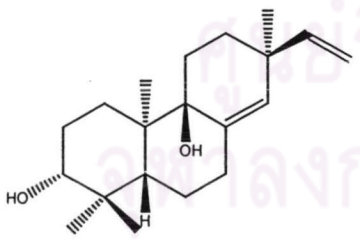

oryzalexin E

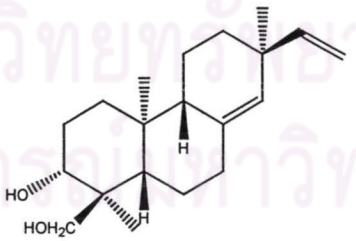

oryzalexin F

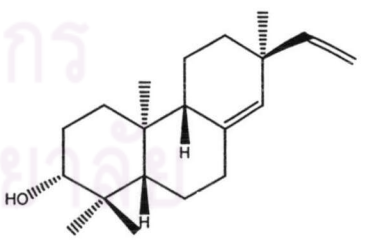

ent-isopimara-8(14),15-dien-3β-ol

Biosynthesis of sandaracopimaradiene structure

Geranylgeranyl pyrophosphate was postulated as a general precursor of cyclic diterpene and converted into (+)-copalyl pyrophosphate, and then sandaracopimaradiene derivatives were obtained.[58,59] The biosynthesis of sandaracopimaradiene derivatives are demonstated in Scheme 3.10.

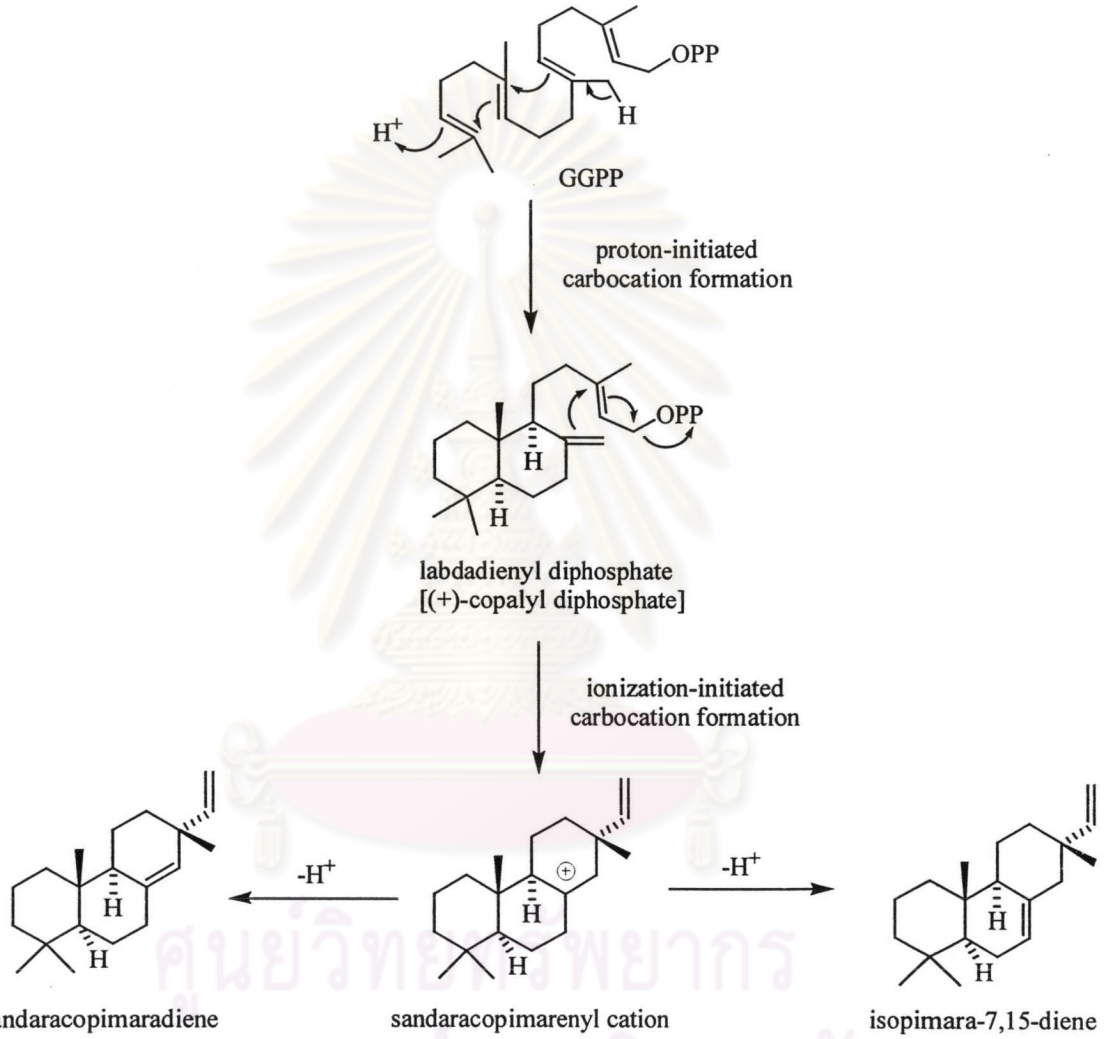

Scheme 3.10 Biosynthesis of sandaracopimaradiene and isopimara-7,15-diene